

# **For Reference**

---

**NOT TO BE TAKEN FROM THIS ROOM**



Ex LIBRIS  
UNIVERSITATIS  
ALBERTAENSIS













THE UNIVERSITY OF ALBERTA

SULFUR ATOM ABSTRACTION

BY METHYL RADICALS AND HYDROGEN ATOMS FROM EPISULFIDES

*by*



MAHMOODA GHANI AHMED

A THESIS

SUBMITTED TO THE FACULTY OF GRADUATE STUDIES AND RESEARCH  
IN PARTIAL FULFILMENT OF THE REQUIREMENTS FOR THE DEGREE  
OF MASTER OF SCIENCE

DEPARTMENT: CHEMISTRY

EDMONTON, ALBERTA

FALL, 1974





TO MY FATHER FOR HIS LOVING CARE





## ABSTRACT

The reactions of methyl radicals, produced by the long wavelength photolysis of azomethane, with propylene episulfide and *cis*-2-butene episulfide yield the corresponding olefins, methane, ethane, dimethyl sulfide, dimethyl disulfide and methyl ethyl diimide. The reaction with *cis*-2-butene episulfide is highly stereoselective, yielding > 80% *cis*-2-butene. Preexponential factors and activation energies were measured for both the desulfurization and the competing hydrogen abstraction reactions.

Hydrogen atoms, produced by the triplet mercury sensitization of hydrogen, react with ethylene episulfide to yield ethylene and hydrogen sulfide. Hydrogen abstraction was not detected. Arrhenius parameters for sulfur abstraction were determined relative to hydrogen abstraction from H<sub>2</sub>S. The activation energy for the desulfurization process is very small.





## ACKNOWLEDGMENTS

I wish to express my most sincere gratitude to Dr. O. P. Strausz who directed this work and provided invaluable assistance by way of discussion, encouragement, and personal attention. Thanks are due to Dr. E. M. Lown who helped me in numerous ways during the preparation of the manuscript.

I am grateful to Dr. E. Jakubowski and Dr. T. Yokota for their advice and technical assistance in the beginning stages of this study.

All the members of the photochemistry group at one time or another helped me in various ways. Thanks are due to Mr. A. Clement for assistance in the preparative work. Also, I would like to mention my next desk neighbour and friend Pavel Neudorfl whose joyful nature made laboratory life so refreshing.

Finally, my profound thanks to Ms. Bonnie Mageau for doing an excellent job in typing the manuscript.





## TABLE OF CONTENTS

	Page
ABSTRACT .....	v
ACKNOWLEDGEMENTS .....	vi
LIST OF TABLES .....	x
LIST OF FIGURES .....	xii
CHAPTER I: INTRODUCTION	
1. Physical and Chemical Properties of Ethylene Oxide and Ethylene Sulfide ....	1
(a) Thermolysis .....	1
(b) Photolysis .....	8
2. Nucleophilic Reactions of Epoxides and Episulfides .....	12
3. Radical Reactions with Epoxides and Episulfides .....	15
(a) General reactions of monovalent radicals .....	15
(b) Radical reactions with epoxides..	18
(c) Radical reactions with episulfides .....	20
4. Aim of the Present Work .....	25





## CHAPTER II: EXPERIMENTAL

1.	High Vacuum System .....	27
2.	Photolysis Assemblies .....	27
	(a) Methyl radical reactions .....	27
	(b) Hydrogen atom reactions .....	29
3.	Photolysis Sources and Actinometry .....	29
4.	Materials .....	32
5.	Analytical Techniques .....	34
6.	Operational Procedure .....	34
	(a) Methyl radical reactions .....	37
	(b) Hydrogen atom reactions .....	37

## CHAPTER III: RESULTS

1.	Methyl Radical Reactions .....	39
	(a) With propylene episulfide .....	39
	(b) With <i>cis</i> -2-butene episulfide .....	42
2.	Hydrogen Atom Reactions with Ethylene Episulfide .....	45
	(a) In the absence of H <sub>2</sub> S .....	49
	(b) In the presence of H <sub>2</sub> S .....	57

CHAPTER IV: DISCUSSION .....	65
------------------------------	----



	Page
CHAPTER V: SUMMARY AND CONCLUSION .....	84
BIBLIOGRAPHY .....	86





# LIST OF TABLES

TABLE		PAGE
I	Thermodynamic Properties of some Molecules and Radicals	2
II	Arrhenius Parameters for the Thermolysis of Episulfides and Epoxides	6
III	Calculated and Observed Arrhenius Parameters for some Reactions Occurring in the $\text{CH}_3 + \text{C}_2\text{H}_4\text{S}$ System	24
IV	Sources of Materials and Purification Procedures	33
V	G.C. Retention Data and Operating Conditions	36
VI	Reactions of Methyl Radicals with Propylene Episulfide. Rates of Product Formation as a Function of Temperature	41
VII	Effect of Conversion on the Product Yields from the Reactions of Methyl Radicals with <i>cis</i> -2-Butene Episulfide	44
VIII	Effect of Temperature on the Product Yields from the Reaction of Methyl Radicals with <i>cis</i> -2-Butene Episulfide	47
IX	Reactions of Hydrogen Atoms with Ethylene Episulfide. Effect of Exposure Time on the Product Yields	50
X	Reactions of Hydrogen Atoms with Ethylene Episulfide. Quantum Yields of $\text{H}_2\text{S}$ and $\text{C}_2\text{H}_4$ as a Function of Exposure Time	52
XI	Reactions of Hydrogen Atoms with Ethylene Episulfide. Rates of formation of $\text{C}_2\text{H}_4$ and $\text{H}_2\text{S}$ as a Function of Episulfide Pressure	54
XII	Quantum Yields of $\text{C}_2\text{H}_4$ and $\text{H}_2\text{S}$ as a Function of Temperature	55
XIII	$\phi_{\text{C}_2\text{H}_4} - \phi_{\text{H}_2\text{S}}$ and $k_{15a}/k_{15}$ from the $\text{H}+\text{EES}$ Reaction	58
XIV	Effect of $\text{H}_2\text{S}$ Pressure on $\phi_{\text{C}_2\text{H}_4}$ in the $\text{H}+\text{EES} + \text{H}_2\text{S}$ System	60



TABLE		PAGE
XV	Slope and Intercept Values from $(\phi_{\text{C}_2\text{H}_4} - k_{15a}/k_{15})^{-1} = 0.5 + k_{17}[\text{H}_2\text{S}]/k_{14}[\text{EES}]$ Plots	62
XVI	Arrhenius Parameters for Some Atom Transfer Reactions	74
XVII	Arrhenius Parameters for Hydrogen Abstraction by Methyl Radicals	75
XVIII	Entropies and Energies of Activation, and Preexponential Factors for Some Metathetical Reactions of Hydrogen Atoms and Methyl Radicals	81





## LIST OF FIGURES

FIGURE	Page
1. The High Vacuum System	28
2. The Photolytic Assembly	30
3. The Analytical System	35
4. Arrhenius Plot for S-Abstraction and H-Abstraction from Propylene Episulfide by Methyl Radicals	42
5. Effect of Reaction Time on the <i>cis</i> -Butene/ <i>trans</i> -Butene Ratio from the Reaction of Methyl Radicals with <i>cis</i> -2-Butene Episulfide	45
6. Arrhenius Plot for S-Abstraction and H-Abstraction from <i>cis</i> -2-Butene Episulfide by Methyl Radicals	48
7. Effect of Exposure Time on the Product Yields of the Hydrogen Atom Reactions with Ethylene Episulfide	51
8. $\gamma = (\phi_{C_2H_4} - k_{15}/k_{15a})^{-1}$ plot against $[H_2S]/[EES]$	61
9. Arrhenius Plot for S-Abstraction from Ethylene Episulfide by H-Atoms	63
10. Schematic Potential Energy Diagram for the Forward and Reverse Processes in the $CH_3 + cis\text{-}2\text{-Butene}$ Episulfide Reaction	68
11. EHMO Potential Energy Curves for the Reaction of Methyl Radicals with Ethylene Episulfide	72
12. Entropy Changes Associated with Metathetical Reactions of H-Atoms and $CH_3$ -Radicals with $H_2S$ and $C_2H_4S$	82



## CHAPTER I

## INTRODUCTION

# 1. Physical and Chemical Properties of Ethylene Oxide and Ethylene Sulfide.

Cyclopropane is the most commonly cited model compound in the development of modern unimolecular rate theories, inasmuch as its physical and chemical properties, and in particular its kinetics of homogeneous decomposition, are well defined. In contrast, the properties of small ring systems containing heteroatoms, such as ethylene oxide or ethylene sulfide, have been relatively little explored. What has emerged however, is that substitution of sulfur for oxygen confers entirely different properties and reactivities on the molecule and these are not solely attributable to the presence of d-orbitals on sulfur. Some thermodynamic properties of ethylene oxide and ethylene sulfide are summarized in Table I along with those of other species pertinent to this work.

## (a) Thermolysis


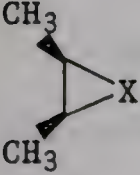
The thermolysis of ethylene oxide produces acetaldehyde, methane, CO and hydrogen as major products<sup>1</sup>. The decomposition is unimolecular and is not affected by the presence of large pressures of propylene. The initial step is believed to be C-O cleavage, followed by isomerization





TABLE I

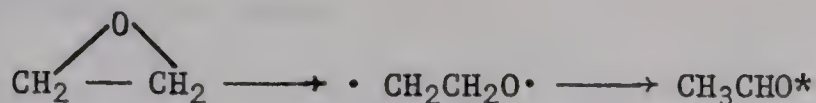
Thermodynamic Properties<sup>a</sup> of Some Molecules and Radicals

Species	$\Delta H_f$		$\Delta H_f (\cdot CH_2CH_2X\cdot)^b$		$D(C-X)^b$	
	X=O	X=S	X=O	X=S	X=O	X=S
 X	-12.19 <sup>c</sup>	19.3 <sup>d</sup>	38.1	71.3	50.3	52.0
	-	-2.73 <sup>d</sup>				
CH <sub>3</sub> X	3.5 <sup>e</sup>	29 <sup>f</sup>				
CH <sub>3</sub> XC <sub>2</sub> H <sub>5</sub>	-	-14.22 <sup>f</sup>				
CH <sub>3</sub> X CH(CH <sub>3</sub> )CH <sub>2</sub> CH <sub>3</sub>	-	-26.41 <sup>f</sup>				
CH <sub>3</sub>	34.0 <sup>e</sup>					
C <sub>2</sub> H <sub>4</sub>	12.5 <sup>e</sup>					
C <sub>3</sub> H <sub>6</sub>	4.9 <sup>e</sup>					
<i>cis</i> -2-C <sub>4</sub> H <sub>8</sub>	-1.36 <sup>e</sup>					

<sup>a</sup> in kcal mole<sup>-1</sup>;<sup>b</sup> S. W. Benson, J. Chem. Phys., 34, 521 (1961);<sup>c</sup> P. Gray and A. Williams, Trans. Far. Soc., 55, 760 (1959).<sup>d</sup> H. Mackle and P. A. G. O'Hare, Tetrahedron, 19, 961 (1963);<sup>e</sup> S. W. Benson, Thermochemical Kinetics, Wiley, New York, 1968;<sup>f</sup> D. H. Fine and J. B. Westmore, Can. J. Chem., 48, 395 (1970).



of the biradical intermediate to an excited acetaldehyde molecule which can contain up to 85 kcal/mole excess energy<sup>1,2</sup>:

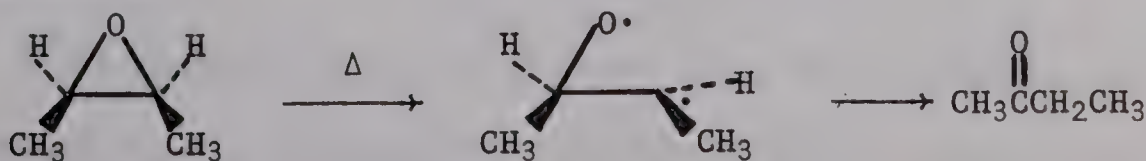


The hot acetaldehyde molecule may then be collisionally stabilized or decompose via a free radical route:



The overall rate constant<sup>1</sup> for the disappearance of ethylene oxide is given by  $k = 10^{14.13} \exp(-56,900/RT) \text{ sec}^{-1}$  and the experimental activation energy can be correlated with the predicted exothermicity of the initial C-O bond cleavage process<sup>2</sup>.

The thermal decomposition of propylene oxide<sup>2,3</sup> and *cis*- and *trans*-2,3-butene oxide<sup>4</sup> are also initiated by first order homogeneous C-O bond cleavage and in the butene oxide decomposition C-C bond rupture also occurs. Although the butene oxide system is complicated by the occurrence of radical processes constituting about 20% of the total primary decomposition, it was possible to establish the modes of formation of most of the observed products and obtain Arrhenius parameters for the reactions. The major product, from either the *cis*- or *trans*-isomer, is 2-butanone which arises from C-O cleavage followed by H-atom shift:

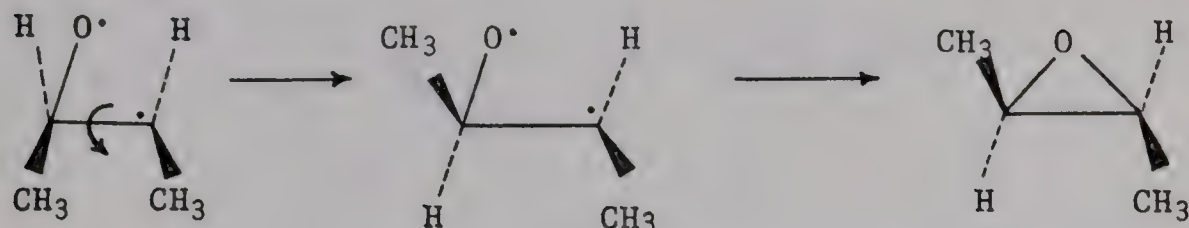


$$k = 10^{13.60} \exp(-56320/RT) \text{ sec}^{-1}$$



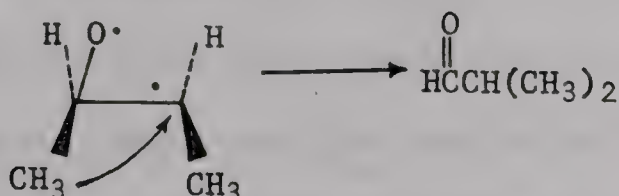


*Cis-trans* isomerization also takes place, although at a relatively slow rate:



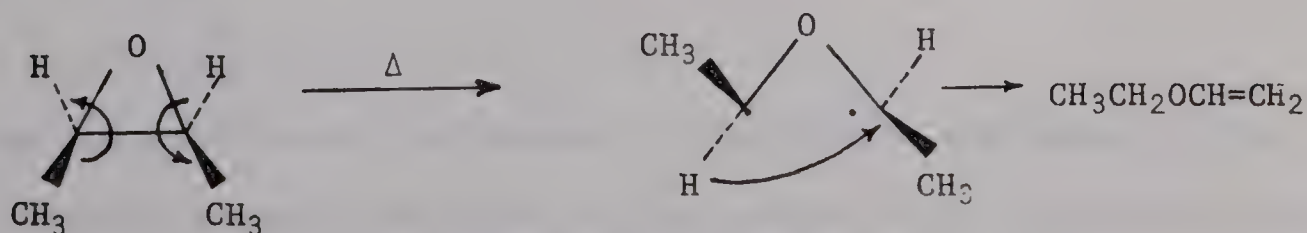
$$k = 10^{14.59} \exp(-61,830/RT) \text{ sec}^{-1}$$

Isobutyraldehyde is formed exclusively from the *cis*-epoxide via  $\text{CH}_3$  group shift:



$$k = 10^{12.99} \exp(-55,970/RT) \text{ sec}^{-1}$$

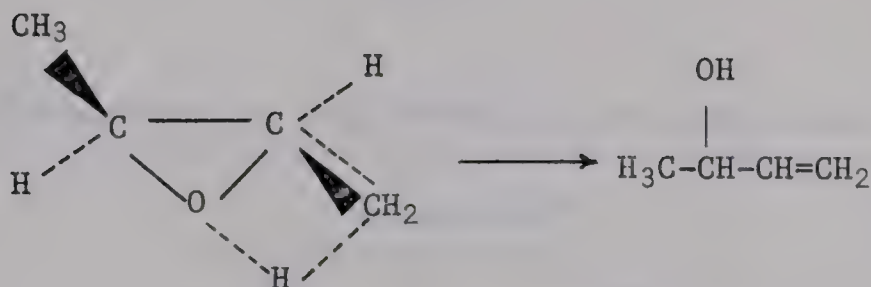
Carbon-carbon cleavage also takes place although to a minor extent and gives rise to ethyl vinyl ether. The rate of this reaction is 12 times faster from the *cis*-epoxide, presumably because the required 1,4 hydrogen shift is much more facile in the *trans*-biradicals preferentially formed, according to the Woodward-Hoffmann rule, from the *cis*-epoxide:



$$k = 10^{12.94} \exp(-55,230/RT) \text{ sec}^{-1}$$

3-Butene-2-ol was also observed as a minor product. It could be formed via 1,4 hydrogen shift in the biradical, but the observed Arrhenius parameters are more compatible with a concerted process:

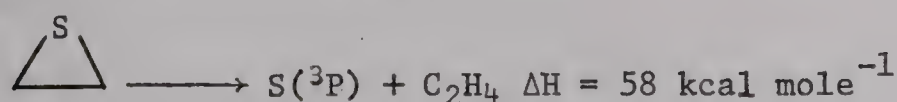




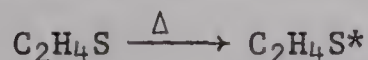
$$k = 10^{12.18} \exp(-53,990/RT) \text{ sec}^{-1}$$

The Arrhenius parameters for the unimolecular decompositions of ethylene, propylene and butene oxides are summarized in Table II.

In contrast, the thermolyses of ethylene, propylene and butene episulfides below 250°C produce polymeric sulfur and the corresponding olefins in nearly quantitative yields<sup>5,6</sup>. The reactions are first order at high pressures and since the activation energies in each case are significantly smaller than either the C-S bond dissociation energies (cf Tables I and II) or the endothermicities required for the hypothetical unimolecular processes e.g.



the overall decomposition must be bimolecular:



The energized episulfide molecule is believed to correspond to the calculated lowest non-vertical triplet state, which is slightly ring opened ( $\angle \text{CCS} \sim 100^\circ$ ) and in which there is a substantial energy





TABLE II

Arrhenius Parameters for the Thermolysis of Episulfides and Epoxides

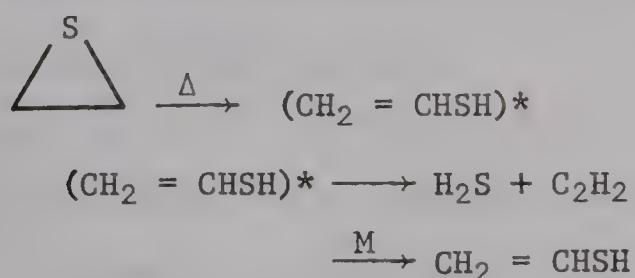
	episulfide <sup>a</sup>		epoxide	
	$E_a$ (kcal mole <sup>-1</sup> )	$\log A$ (cc mole <sup>-1</sup> sec <sup>-1</sup> )	$E_a$ (kcal mole <sup>-1</sup> )	$\log A$ (cc mole <sup>-1</sup> sec <sup>-1</sup> )
ethylene	40.2	12.52	56.9 <sup>b</sup>	14.13 <sup>b</sup>
propylene	38.7	12.57	58 <sup>c</sup>	14.1 <sup>c</sup>
<i>trans</i> -2-butene	35.7	12.08	59.3 <sup>d</sup>	14.24 <sup>d</sup>
<i>cis</i> -2-butene	-	-	56.3 <sup>d</sup>	13.6 <sup>d</sup>

<sup>a</sup> reference 6<sup>b</sup> reference 1<sup>c</sup> reference 3<sup>d</sup> reference 4



barrier to rotation of the terminal methylene group. The existence of this rotational energy barrier is evidenced by the high degree of stereoselectivity observed in the pyrolysis of *cis*- and *trans*-2-butene episulfides, which afforded 90% *cis*- and 96.2% *trans*-2-butene, respectively. In contrast to the epoxide decomposition however, the rates of decomposition of episulfides are strongly suppressed in the presence of olefins, which apparently quench the triplet state episulfides very efficiently. The resulting kinetics are very complex and require further elucidation.

At higher temperatures an additional decomposition route becomes operative. Qualitative observations are best explained by a unimolecular isomerization to vinyl mercaptan which may subsequently decompose to hydrogen sulfide and acetylene or be collisionally stabilized,



The drastic alteration in the mode of decomposition upon substituting sulfur for oxygen may be related to two causes. Firstly, the exothermicity of the epoxide - aldehyde rearrangement is much greater than the hypothetical episulfide-thiocarbonyl isomerization. This may be inferred from a comparison of the C=O and C=S bond strengths in formaldehyde and thioformaldehyde<sup>7</sup>,  $D(\text{H}_2\text{C}=\text{O}) = 173$  and  $D(\text{H}_2\text{C}=\text{S}) = 124$  kcal mole<sup>-1</sup> and the fact that the C-O and C-S bond strengths in



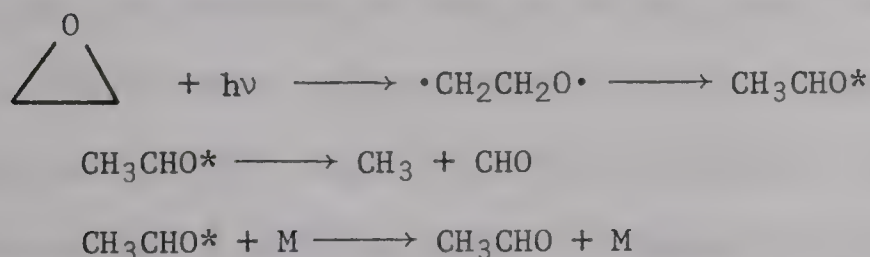


epoxides and episulfides are nearly equal (Table I). Secondly, the d-orbitals on sulfur always lower the energies of the excited states and owing to heavy atom perturbation the triplet state episulfide is accessible in thermolysis, whereas the triplet state of epoxides on the other hand lies at prohibitively high energies<sup>8</sup>.

### (b) Photolysis

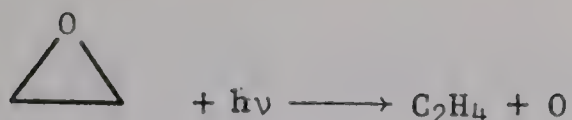
The lowest energy absorption in ethylene oxide occurs at 1713 Å<sup>o</sup> and at high pressures continuous absorption extends up to about 2120 Å<sup>o</sup><sup>9</sup>. The transition is likely  $n \rightarrow \sigma^*$ .

Conventional photolysis of ethylene oxide<sup>10</sup> leads to the same major products as observed in thermolysis, namely CO, CH<sub>4</sub> and H<sub>2</sub>. Acetaldehyde was also formed, but to a minor extent. Since the absorption spectrum of acetaldehyde was observed at long exposures<sup>9</sup> it seems likely that the mechanism for photochemical decomposition is the same as that for thermolysis, i.e.,

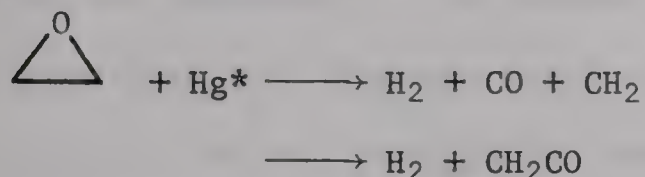


In flash photolysis experiments<sup>11</sup> however, small but significant yields of ethylene were also observed. Since the quantities formed were too large to be accounted for by the disproportionation of methyl radicals, it was proposed that ethylene is formed in a primary molecular process:





The triplet mercury sensitized decomposition of ethylene oxide<sup>12</sup> is similar in many respects to the direct photolysis, and while an unambiguous solution of the complete reaction mechanism was not possible, some important features of the decomposition were brought to light from the inhibiting effects of 1-butene on some of the product yields. For example, the limiting H<sub>2</sub> yield under these conditions corresponds to a molecular mode of formation, possibly via



Substantial amounts of C<sub>2</sub>H<sub>4</sub> were formed in the inhibited reaction, amounting to ca. 30% of the CO and it was demonstrated that the retrievable yields of C<sub>2</sub>H<sub>4</sub>, as well as those of most of the other products, are governed by H-atom reactions. Thus, in the uninhibited reaction, the addition of H-atoms to ethylene is much faster than the rate of abstraction from ethylene oxide, and therefore the true ethylene yields must be much higher than those observed. Unimolecular deoxygenation of ethylene oxide was suggested as the source of C<sub>2</sub>H<sub>4</sub> although some reactions involving CH<sub>2</sub> radicals may also be involved.

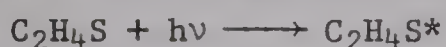
These facts strongly point to the intervention of at least two molecular processes in competition with C-O cleavage, one leading to H<sub>2</sub> and the other to C<sub>2</sub>H<sub>4</sub>. It would therefore be highly desirable to reinvestigate the conventional photolysis of ethylene oxide especially in the presence of radical scavengers.



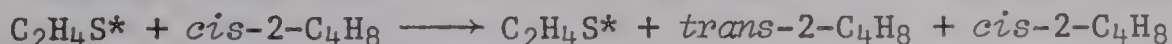


The near UV spectrum of ethylene sulfide<sup>13</sup> is characterized by an intense band at 2600 Å, with an inflection at 2450 Å and continuous absorption below 2200 Å. The lowest energy absorption is believed to arise from a  $b_2^* \leftarrow 3p_x$  (or  $nb_2^* \leftarrow A_1$ ) transition<sup>14</sup>. Semi-empirical SCF (CNDO/2) calculations applied to the UV spectra of cyclic organic sulfides have shown<sup>15</sup> that in the lowest excited states, d-orbital participation is very important.

The gas phase photolysis of ethylene sulfide above 2200 Å produces sulfur and ethylene<sup>16</sup>. The quantum yield of ethylene production is two and decreases with ethylene sulfide pressure to a value of about one. In the presence of *cis*-2-butene the ethylene yields are strongly suppressed and large quantities of *trans*-2-butene are formed. The quantum yield of *cis-trans* isomerization is proportional to the *cis*-2-butene pressure and is approximately 100 times that of  $\phi(C_2H_4)$  at the highest olefin pressure used, 400 torr. A bimolecular mechanism is therefore indicated,



in which the excited episulfide molecule is sufficiently long-lived to participate in a chain isomerization reaction with *cis*-2-butene:



The lifetime of  $C_2H_4S^*$  must be at least  $10^{-5}$  sec in order to engage in this process, and the chain length of isomerization is roughly 100.

Sensitization by biacetyl ( $E_{exc} = 55$  kcal mole<sup>-1</sup>) or benzene ( $E_{exc} = 85$  kcal mole<sup>-1</sup>) led to results which are in accord with the above mechanism.

The alternative mechanism, involving primary extrusion of sulfur atoms,







can be discounted for several reasons. Firstly, the excitation energy in biacetyl is less than the endothermicity of the sulfur extrusion process, yet  $\phi(C_2H_4)$  is the same as in the direct photolysis. Secondly, when sufficiently large quantities of olefin are added to the system such that the rate of addition of sulfur atoms to the double bond,



can compete with the  $S + C_2H_4S$  reaction, only minute traces of the olefin episulfide were recovered. Therefore, the concentration of sulfur atoms in the system must be negligibly small. Finally, the existence of a long lived excited episulfide state which can promote *cis-trans* isomerization in 2-butene via a chain process has been unequivocally demonstrated in thermolysis experiments and in studies of S-atom addition to *cis*-2-butene.

The nature of the excited episulfide state formed in photolysis cannot be defined at present. The strong quenching effect of olefins suggests a triplet state but it must be, at least initially, of higher energy than the triplet state populated by intersystem crossing in thermolysis.

Bearing these results in mind, and recalling that ethylene appears to be a significant product in the direct and sensitized photolysis of ethylene oxide, a similar bimolecular reaction involving an excited ethylene oxide molecule may be occurring in this system; such a process, if it indeed occurs, is a minor one but can be theoretically of great interest.

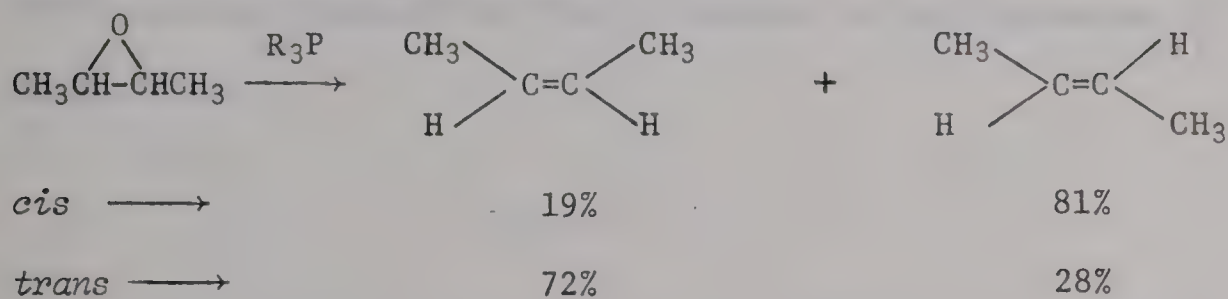




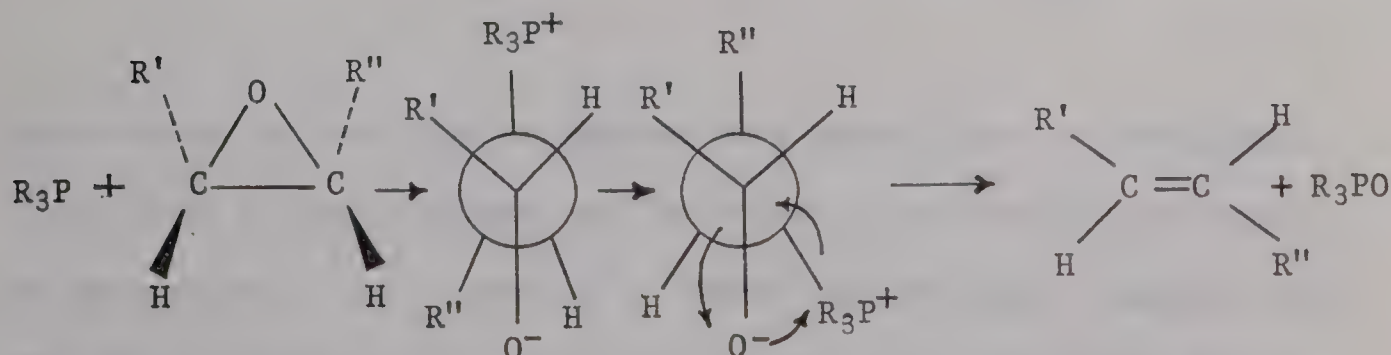
## 2. Nucleophilic Reactions of Epoxides and Episulfides.

The characteristic differences in the thermal and photochemical behavior of epoxides and episulfides are also manifested in their chemical reactions with nucleophiles, which lead to extrusion of the heteroatom.

The deoxygenation of epoxides by tertiary phosphines yields as the predominant product an olefin having a configuration opposite to that of the starting epoxide:<sup>17,18</sup>



Presumably, the reaction occurs by nucleophilic attack of the tertiary phosphine at an epoxide carbon atom, thus affording a betaine intermediate which, after rotation of the central carbon-carbon bond by 180°, collapses with the liberation of t-phosphine oxide and olefin:

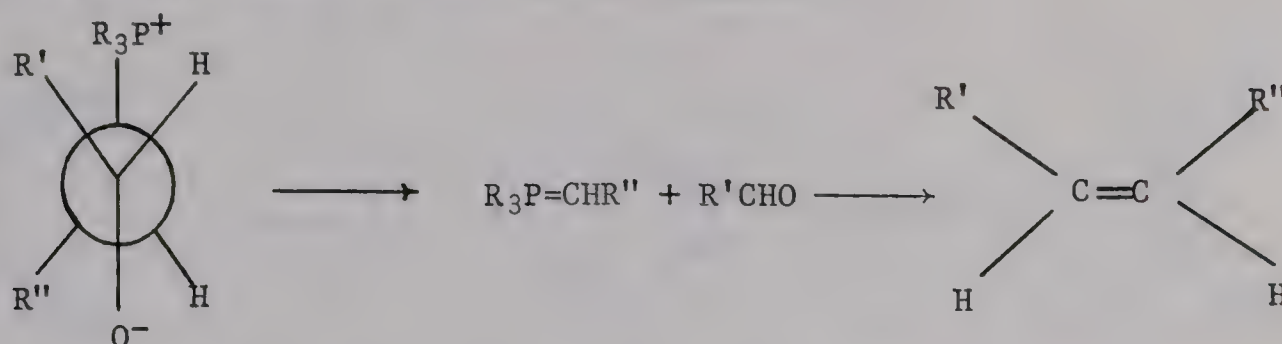


The small yields of the other olefin isomer probably arise from a minor reaction pathway by the betaine to form an ylid and acetaldehyde; a Wittig -type recombination of these two moieties would be expected to

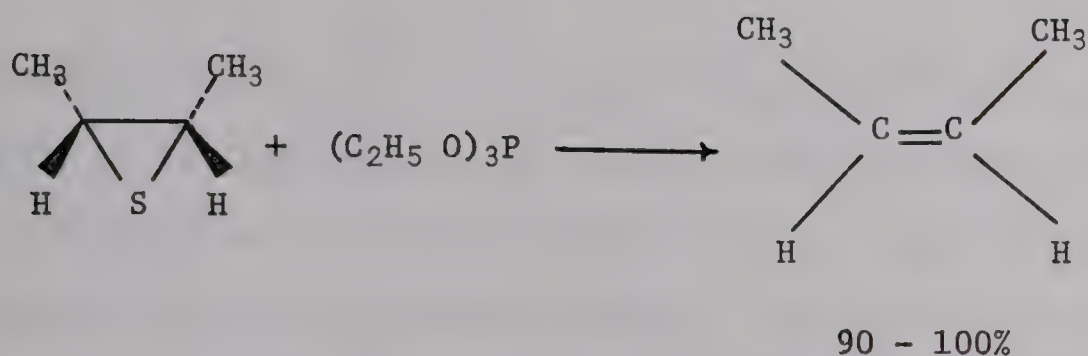




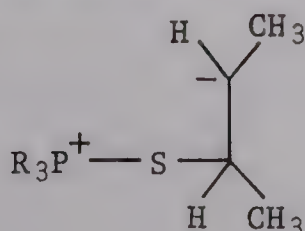
lead to a certain amount of *cis*-olefin formation<sup>19,20</sup>.



In contrast, treatment of episulfides with tertiary phosphines<sup>21,22</sup>, phosphites<sup>22,24</sup> or alkyl or aryl lithium reagents<sup>23,25</sup> is greater than 90% stereoselective and the olefin retains the configuration of the heterocycle:

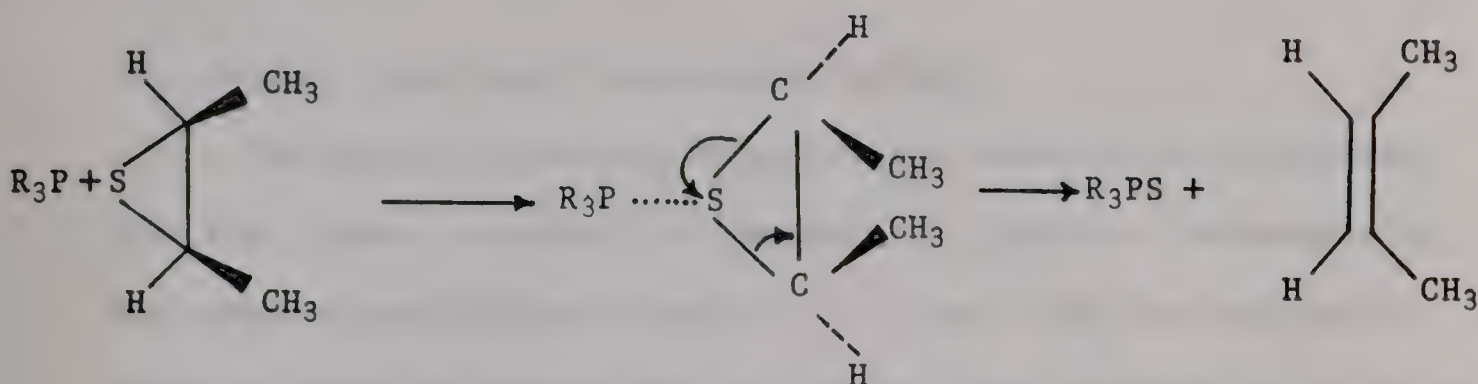


The reaction of tertiary phosphines with episulfides is bimolecular, first order in each reactant and the rate is unaffected by solvents of varying dielectric constant<sup>21</sup>. These observations, together with the observed high stereoselectivity of the desulfurization reaction, militate against an ionic intermediate such as

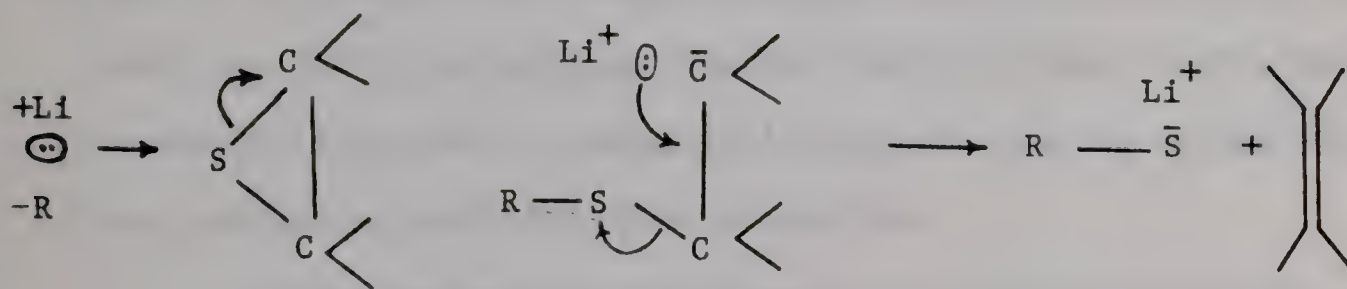




and indicate a concerted mechanism:



The organolithium reaction is not as well defined. It has been postulated<sup>25</sup> to proceed via



but it has been pointed out<sup>26</sup> that in order for the olefin to retain the geometry of the heterocycle, the postulated intermediate must have a very brief lifetime, if indeed it exists at all, a condition which is not compatible with the proposed structure. In any case, the site of attack must be at the sulfur atom in contrast to the organolithium + epoxide reaction where attack at the carbon atom of the ring leads to the formation of alcohols. There are several reasons for this<sup>25</sup>;

- (1) sulfur is more electropositive and polarizable than oxygen;
- (2) the carbon-sulfur dipole is small, and (3) divalent sulfur is known to be susceptible to attack by nucleophilic agents.



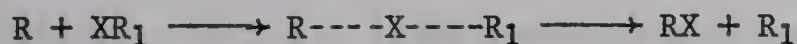


### 3. Radical Reactions With Epoxides And Episulfides

#### (a) General reactions of monovalent radicals

The chemical reactions of monovalent radicals can be classed into four types: transfer (or abstraction), addition, decomposition, and combination-disproportionation. Of these, only the combination reactions occur at a rate close to the collision frequency with little or no activation energy; the others are slower and require a measurable activation energy. The transfer reactions of H atoms and CH<sub>3</sub> radicals have been widely investigated and the resulting kinetic data have been successfully applied to theoretical concepts relating to the microscopic rate processes, which will now be described.

In the simplest transfer reaction, a monovalent atom of a substrate molecule is transferred to a monovalent radical via an abstractive process:



Most of the transfer reactions of atoms have frequency factors of the order of  $10^{11} \text{ l mole}^{-1} \text{ sec}^{-1}$  corresponding to a collision efficiency of about 0.1<sup>27</sup>. Those for small radicals are  $\sim 10^8$  indicating larger entropy contributions in the activated state.

Transfer reactions are generally envisaged as passing through a transition state in which the RX bond is partially formed and the R<sub>1</sub>X bond is partially ruptured. Since the experimentally measured activation energies are an order of magnitude smaller than the R<sub>1</sub>X bond energies, it must be concluded that the energy released



upon formation of the new RX bond partially provides the energy required for  $R_1X$  rupture. From the experimentally observed dependence of the activation energy ( $E_a$ ) on the  $R_1X$  bond energy, Evans and Polanyi<sup>28,29</sup> derived the following empirical relation between  $E_a$  and  $\Delta H$ , the heat of reaction:

$$\Delta E_a = \alpha \Delta H$$

where  $\alpha$  is a constant within a homologous series. In some cases there is good agreement between calculated and experimental activation energies, but wider applications of this relation are severely limited in that it predicts negative activation energies for highly exothermic reactions whereas, in practice,  $E_a$  becomes zero as  $\Delta H$  becomes sufficiently large.

To date, the most successful method of predicting activation energies is the Bond Energy Bond Order (BEBO) method developed by H.S. Johnston<sup>30,31</sup>. The method is purely empirical and does not rely on kinetic data; the only input parameters are experimental values of bond dissociation energies and bond lengths, and calculated values of bond orders and bond energy indices<sup>31</sup>. Thus for the model reaction



the relevant terms are denoted by:



$R_1$	$R_2$	$R_3 = R_1 + R_2$	bond lengths in the activated complex
$n$	$m$		bond order
$p$	$q$		bond energy index





$R_{1s}$              $R_{2s}$             single bond length in stable molecule

$E_{1s}$              $E_{2s}$             single bond energy

Assuming that the path of lowest energy from reactants to products is obtained when the sum of the bond orders is unity, i.e.,

$$n + m = 1$$

the potential energy of transition state formation is given by

$$V = E_{1s}(1-n^p) - E_{2s}(1-m^q) + V_{tr}$$

where  $V_{tr}$  is the triplet repulsion term arising from the fact that the electron spins on atoms A and B are parallel, and is calculated from an anti-Morse function. Usually,  $V$  is calculated point by point for values of  $n_1$  between 0 and 1, adjusting the value of  $n_2$  such that  $V$ , which then corresponds to the activation energy, is a minimum.

Activation energies for simple hydrogen atom and methyl radical transfer reactions computed by this method generally agree with experimental values to within 2-3 kcal mole<sup>-1</sup> <sup>31</sup>. Successful application of the method to some systems however, may be restricted for the following reasons:

- (1) reliable bond energies and distances may not be available, for example in the silanes;
- (2) the transition state was originally based on the  $H + H_2$  reaction, a 3-atom complex. When the abstractable species is part of a complex (e.g., cyclic) molecule the assumed model is greatly oversimplified;
- (3) the bond energy indices calculated from empirical relations, may differ considerably from those obtained by "best fits" to kinetic





data and in such cases the correct choice may not be immediately obvious.

The method has also been applied to abstraction of multivalent atoms such as oxygen. Here, however, spin angular momentum can only be conserved in the reaction if the O-atom is abstracted in its lowest  $^1D_2$  state. It was shown<sup>32</sup> that if the singlet-triplet excitation energy is added to the dissociation energies of the bonds being formed and ruptured, good agreement between the observed and calculated activation energies was obtained.

Preexponential factors can also be estimated as lower limits, from thermochemical data. The method<sup>33</sup> is based on the assumption that the activated state is a rigid complex whose entropy can be calculated by comparison with analogous molecules.

The various translational, rotational, vibrational, spin and symmetry contributions to the entropy can be evaluated from standard tables. The preexponential factor is then obtained from

$$A = \frac{ekT}{h} e^{\Delta S^\ddagger/R}$$

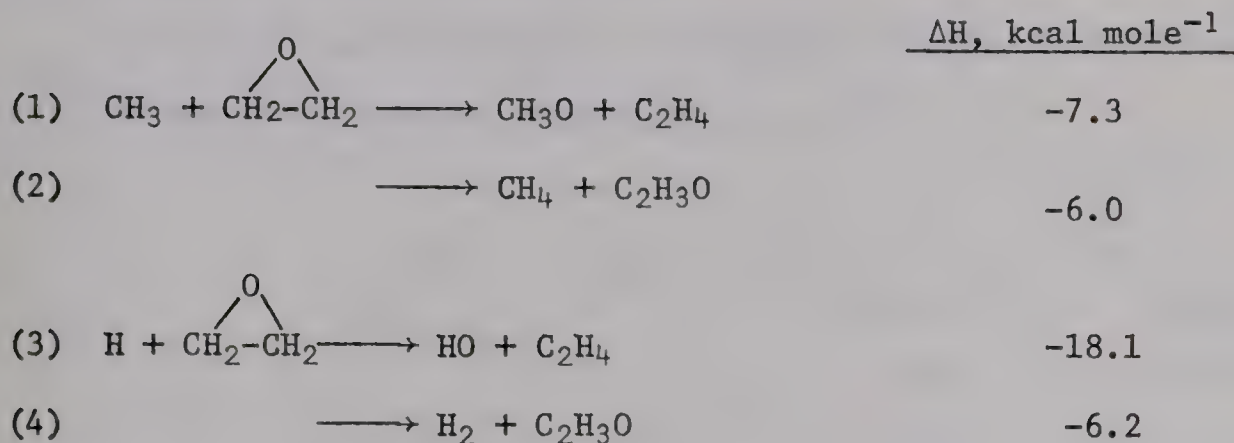
where  $\Delta S^\ddagger$  is the calculated lower limit of the entropy change and the other terms have their usual significance. Comparison with the experimental value of A can then yield valuable information regarding the structure of the activated complex.

#### (b) Radical reactions with epoxides

The enthalpies associated with the hypothetical H and O-atom transfer reactions from ethylene oxide to H or  $CH_3$  radicals are listed



below (*cf.* Table I):



It is immediately apparent that, from the thermodynamic standpoint, the hitherto unknown deoxygenation reaction by a monovalent radical is at least as favorable as the classical H-abstraction reaction. Yet only isolated reports of radical reactions with epoxides are available and it appears that H-abstraction is the only important primary process.

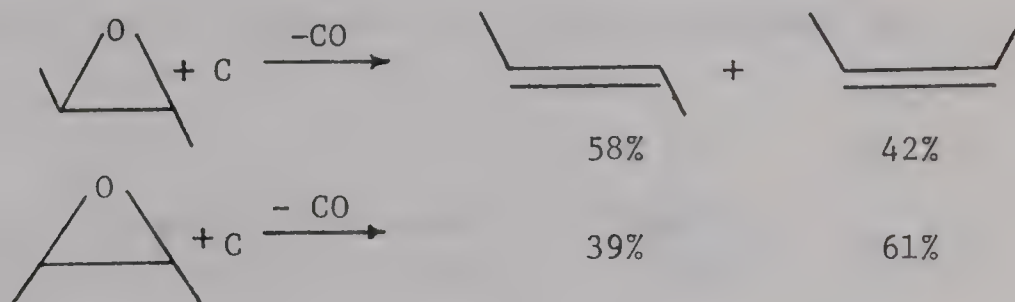
Early work<sup>34,35</sup> on the reactions of  $\text{CH}_3$  radicals with ethylene oxide indicated that O-abstraction did not occur. A recent investigation of the  $\text{CF}_3$  + ethylene oxide reaction<sup>36</sup> led essentially to the same conclusion and the Arrhenius parameters for the reaction were determined to be  $\log A = 12.5$  ( $\text{cc mole}^{-1} \text{ sec}^{-1}$ ) and  $E_a = 11.0 \text{ kcal mole}^{-1}$ . The earlier data of Phibbs and Darwent<sup>34</sup> for the  $\text{CH}_3$  + ethylene oxide reaction were recalculated, and a somewhat higher value of  $E_a$ ,  $10.1 \text{ kcal mole}^{-1}$  was obtained. The authors suggest that the true activation energy should be substantially higher than this, perhaps in the neighbourhood of  $14 \text{ kcal mole}^{-1}$ .



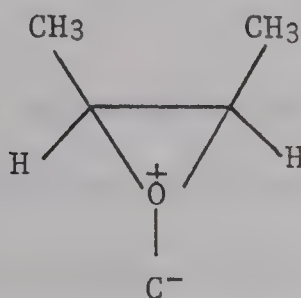


Similarly, the reactions of H atoms with ethylene oxide<sup>37</sup> appear to involve only H-abstraction.

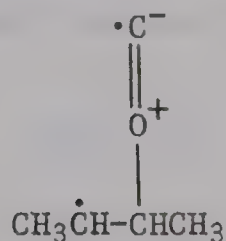
In contrast, epoxides are deoxygenated by atomic carbon to yield olefins in a non-stereospecific manner<sup>38</sup>:



The primary intermediate is postulated to be an ylid



which must subsequently rearrange to a linear biradical-ion



in order to account for the non-stereospecificity of the reaction.

### (c) Radical reactions with episulfides

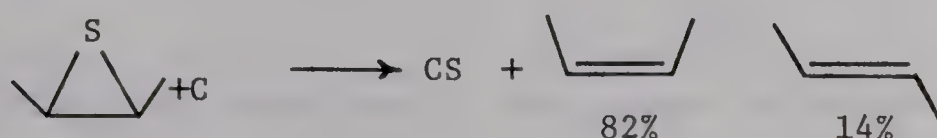
Until recently, only two isolated reports of radical reactions with episulfides were available in the literature. A brief mention<sup>39</sup>



of the *t*-butoxy + propylene sulfide reaction stated that H-abstraction was the only observable process:



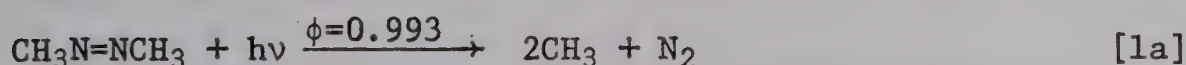
Plonka and Skell<sup>40</sup> showed that carbon atoms desulfurize *cis*-1,2-dimethyl episulfide and a high degree of stereoselectivity was observed:



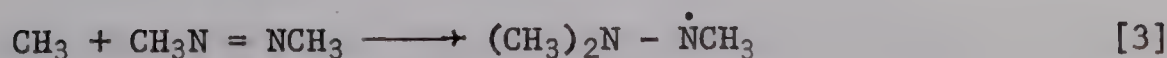
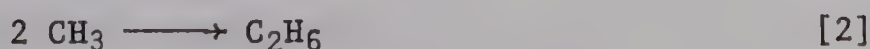
Unfortunately, neither the rate parameters nor the spin state of the carbon atom were estimated.

The reactions of singlet and triplet state sulfur atoms, produced from the photolysis of COS, have been well documented<sup>41</sup>. As an integral part of the continuing studies of S-atom reactions originating from this laboratory, the reactions of methyl radicals with COS and ethylene episulfide were then explored<sup>42</sup>.

Methyl radicals were produced from the photolysis of azomethane<sup>43,44</sup>:



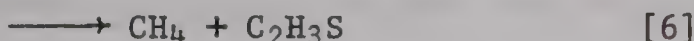
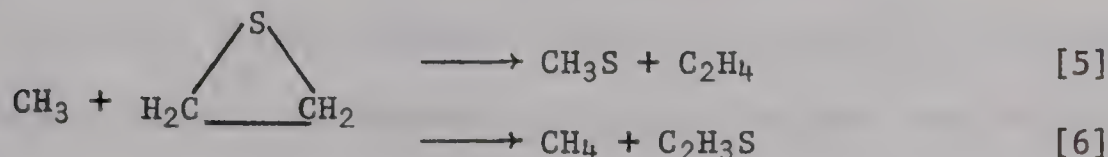
Since elementary rate constants have been determined for the following secondary radical reactions<sup>45</sup>,



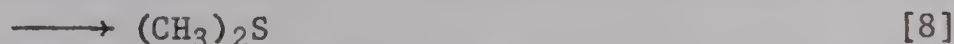
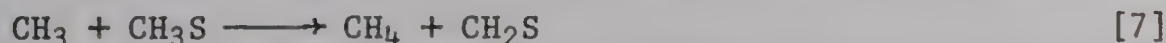




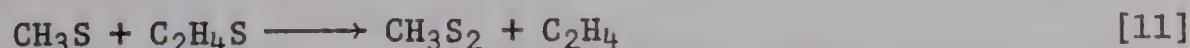
the  $\text{C}_2\text{H}_6$  yields represent a quantitative reference for the determination of the rate constant for the competing reaction of methyl radicals with ethylene episulfide:



The photolysis of azomethane in the presence of ethylene episulfide gave rise to  $\text{N}_2$ ,  $\text{C}_2\text{H}_4$ ,  $\text{CH}_3\text{SCH}_3$  and  $\text{CH}_3\text{SSCH}_3$  along with smaller yields of  $\text{CH}_4$ ,  $\text{C}_2\text{H}_6$  and methylethyldiimide. Small amounts of NO strongly suppressed the product yields, indicating that they originate from free radical precursors. The overall reaction can be described in terms of the elementary processes [1] - [6], followed by



A temperature study however, indicated that an additional  $\text{C}_2\text{H}_4$ -producing reaction becomes important at high temperatures. By analogy with the  $\text{S} + \text{C}_2\text{H}_4\text{S} \longrightarrow \text{S}_2 + \text{C}_2\text{H}_4$  reaction which occurs at a rate close to the collision frequency<sup>46</sup> the excess  $\text{C}_2\text{H}_4$  probably arises from an analogous sulfur abstraction by methyl thiyl radicals:



The  $\text{C}_2\text{H}_4$  yields were therefore corrected in order to reflect step [5]





only, and the rate parameters for the various elementary processes occurring in the  $\text{CH}_3 + \text{C}_2\text{H}_4\text{S}$  system are summarized in Table III.

Activation energies and preexponential factors were also estimated by the BEBO and Benson's method<sup>33</sup>, respectively, and are also listed in Table III.

The major primary process observed in the  $\text{CH}_3 + \text{C}_2\text{H}_4\text{S}$  system is a unique abstraction reaction wherein a divalent atom is abstracted by a monovalent radical. This is in striking contrast to the  $\text{CH}_3$ ,  $\text{CF}_3$  or  $\text{H} + \text{C}_2\text{H}_4\text{O}$  system, where H-abstraction is the only major mode of attack. Since the enthalpy changes for the analogous reactions:



are not sufficiently disparate to account for the occurrence of S-atom abstraction, BEBO calculations were carried out for the activation energies. For the epoxide case, the predicted activation energies are 40 and 0  $\text{kcal mole}^{-1}$ , with and without the inclusion of the singlet-triplet excitation energy to  $\text{D}(\text{C}-\text{O})$ , respectively. It is expected however, that the spin conservation requirement in the case of oxygen would be fairly stringent and the non-occurrence of O-atom abstraction by  $\text{CH}_3$  radicals is undoubtedly due to the prohibitively high activation energy for such a process. For S-atom abstraction however, the experimental activation energy lies about midway between the calculated values (cf. Table III). This is reasonable if, as is probably the case, there is a partial relaxation of the spin angular momentum selection



TABLE III

Calculated and Observed Arrhenius Parameters for Some Reactions Occurring in the  $\text{CH}_3 + \text{C}_2\text{H}_4\text{S}$  System

Reaction	$\log A(\text{cc mole}^{-1} \text{ sec}^{-1})$		$E_a, \text{ kcal mole}^{-1}$	
	Obs.	Calc.	Obs.	Calc.
$\text{CH}_3 + \text{C}_2\text{H}_4\text{S} \longrightarrow \text{CH}_3\text{S} + \text{C}_2\text{H}_4$	$10.85 \pm 0.48$	$> 10$	$6.7 \pm 0.8$	$14^a \quad 0^b$
$\text{CD}_3^c + \text{C}_2\text{H}_4\text{S} \longrightarrow \text{CD}_3\text{S} + \text{C}_2\text{H}_4$	$10.77 \pm 0.64$		$6.5 \pm 1.0$	
$\text{CD}_3^c + \text{C}_2\text{H}_4\text{S} \longrightarrow \text{CD}_3\text{H} + \text{C}_2\text{H}_3\text{S}$	$11.34 \pm 0.60$		$9.5 \pm 1.0$	
$\text{CH}_3\text{S} + \text{C}_2\text{H}_4\text{S} \longrightarrow \text{CH}_3\text{S}_2 + \text{C}_2\text{H}_4$	$\sim 11.5$		$\sim 8.8$	

<sup>a</sup> Computed with the inclusion of the singlet-triplet excitation energy,  $26.4 \text{ kcal mole}^{-1}$ , in  $\text{D}(\text{C-S})$ <sup>b</sup> Computed using  $\text{D}(\text{C-S})$  only<sup>c</sup> From the photolysis of  $\text{CD}_3\text{N} = \text{NCD}_3$





rule owing to heavy atom perturbation.

The A factor for the  $\text{CH}_3 + \text{C}_2\text{H}_4\text{S}$  reaction was also calculated by Benson's method<sup>33</sup> and the somewhat smaller value indicates that there is some looseness in the transition state.

Methyl radicals also abstract sulfur from carbonyl sulfide, at a rate given by

$$\log k = 11.58 \pm 0.25 - (11,350 \pm 350/RT) (\text{cc mole}^{-1} \text{ sec}^{-1})$$

Again the observed activation energy is midway between the BEBO values.

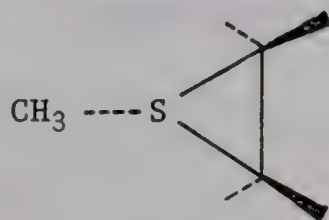
#### 4. Aim of the Present Work.

The desulfurization of ethylene episulfide by methyl radicals is a hitherto unknown reaction and the simplicity of the kinetic treatment of the azomethane-episulfide systems, together with the ease of product analysis, mean that accurate rate data can be derived and thus extend our meagre knowledge of the chemistry of episulfides. It was therefore decided to carry out a systematic study of the reactions of methyl radicals with other episulfides, namely propylene and *cis*-2-butene episulfides, and to establish, in each case, the Arrhenius parameters for S-atom abstraction.

The reaction with 2-butene episulfide is particularly significant since the geometries of the product olefins can be instrumental in defining the nature of the reaction intermediates. Thus if a thiyl



radical intermediate is implicated,  $\text{CH}_3\text{CH} - \dot{\text{C}}\text{HCH}_3$ , one might expect about an equal yield of *cis*- and *trans*- $\text{SCH}_3$  2-butene. A one step concerted complex on the other hand



would lead to only one olefin having the same configuration as the episulfide.

In order to ascertain whether S-atom abstraction from episulfides is a characteristic reaction of monovalent radicals, the reactions of hydrogen atoms with ethylene episulfide were also examined, and Arrhenius parameters were determined for some of the elementary reactions.



## CHAPTER II

### EXPERIMENTAL

#### 1. High Vacuum System

A conventional high vacuum system (Fig. 1) consisting of pumps, distillation units, material storage bulbs, Toepler pumps, gas burette and metering units was used. The system was evacuated to  $10^{-6}$  torr with a mercury diffusion pump backed by a Welsh Duoseal mechanical pump. Helium tested Hoke valves, Springham stopcocks with Viton A diaphragms, Teflon plug stopcocks and Delmar mercury float valves were used throughout the system.

Absolute pressures were measured by a McLeod gauge. A Pirani gauge was used to monitor distillations and gas transferences using Pirani tube sensors. For distillation and product fractionation several U-traps and multi-coil traps interconnected by mercury float valves were used. There was also a solid nitrogen trap in the distillation unit.

#### 2. Photolysis Assemblies

##### (a) Methyl radical reactions

The reactions were carried out in a cylindrical quartz cell,





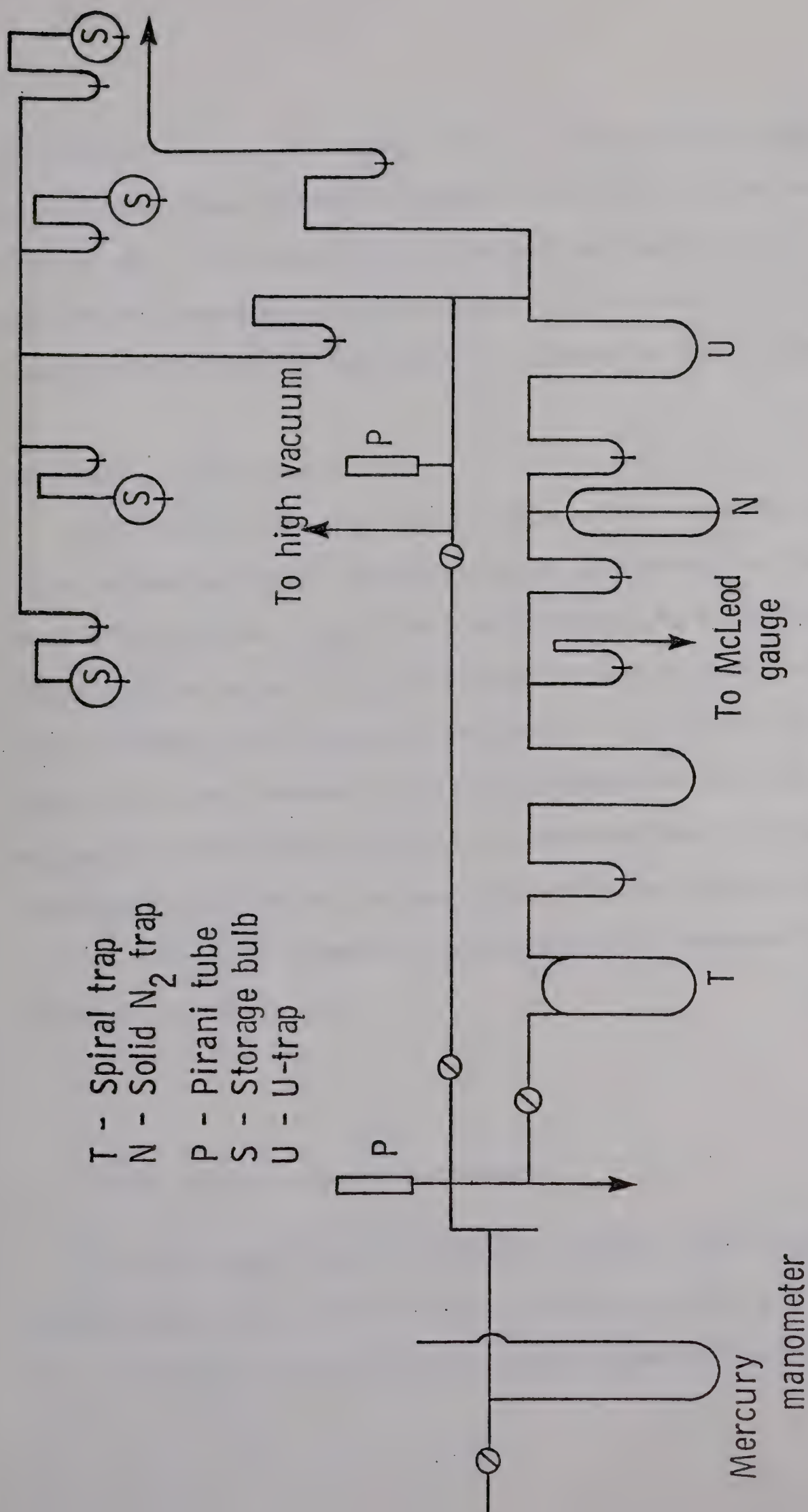


Fig. 1 The high vacuum system



10 cm long 5 cm wide, of volume  $\sim$  190 cc. The cell was enclosed in an aluminum block furnace which was insulated by a 2 cm thickness of glass wool. The temperature of the cell was measured by standardized iron-constantan thermocouples. The reaction cell was connected to the rest of the system by a quartz to pyrex graded seal.

(b) Hydrogen atom reactions

The photolytic assembly was slightly modified for the study of the H-atom reactions. The apparatus is illustrated in Figure 2. The 5 x 10 cm quartz reaction cell was connected to a circulating system in order to provide rapid mixing of reactant gases before and during reaction, and to minimize the amount of deposition of elemental sulfur on the cell window. The fan type circulator was constructed of glass and Teflon, and driven by an induction motor. A small tube containing liquid mercury at room temperature was connected close to the cell. The cell temperature was maintained and measured as described in section 2(a).

### 3. Photolysis Sources and Actinometry

For the methyl radical reactions a Hanovia medium pressure mercury lamp, Model 30620 was used in conjunction with a Kodak Wratten No. 18 A filter in order to limit the effective wavelength to the





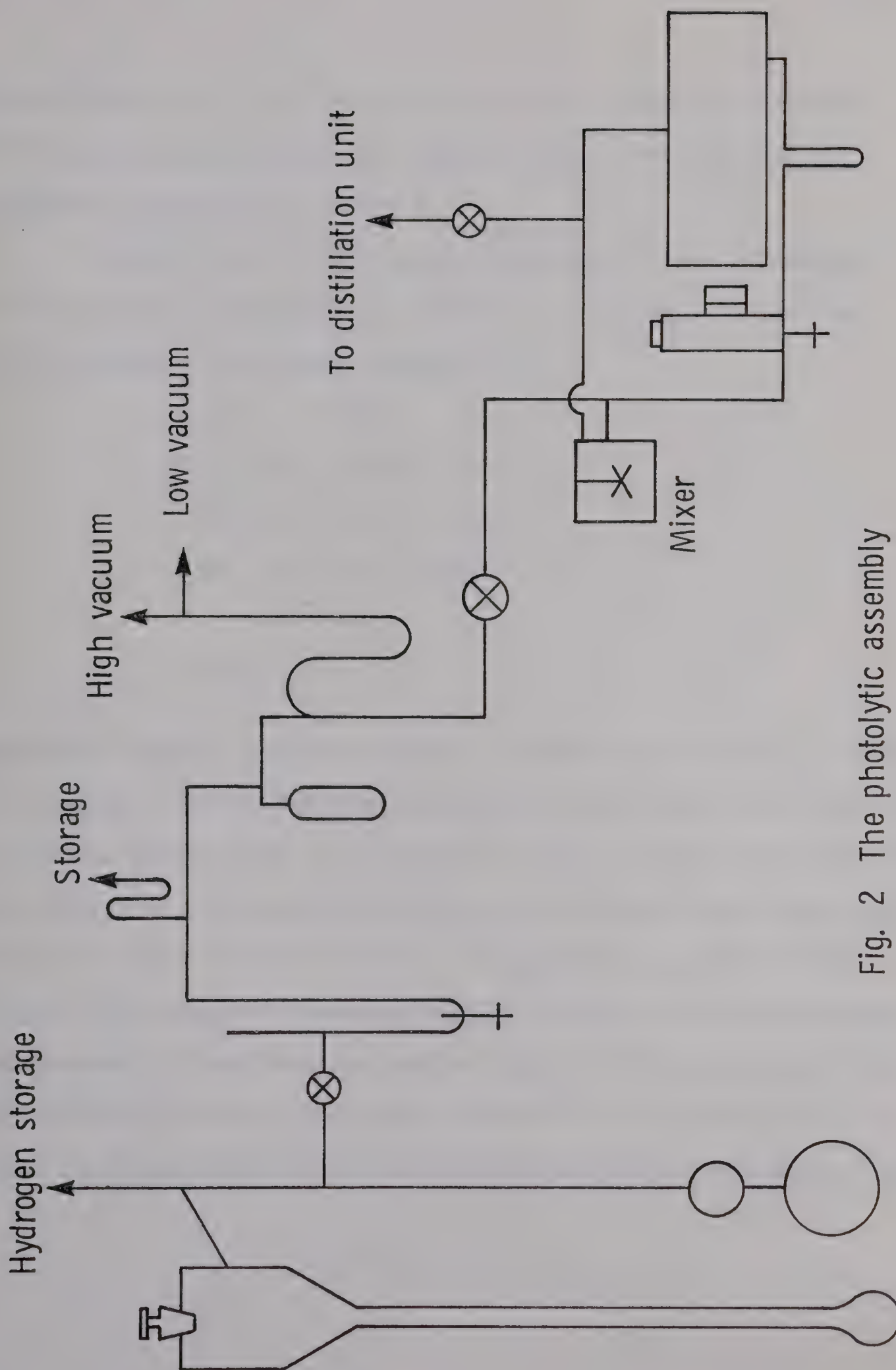
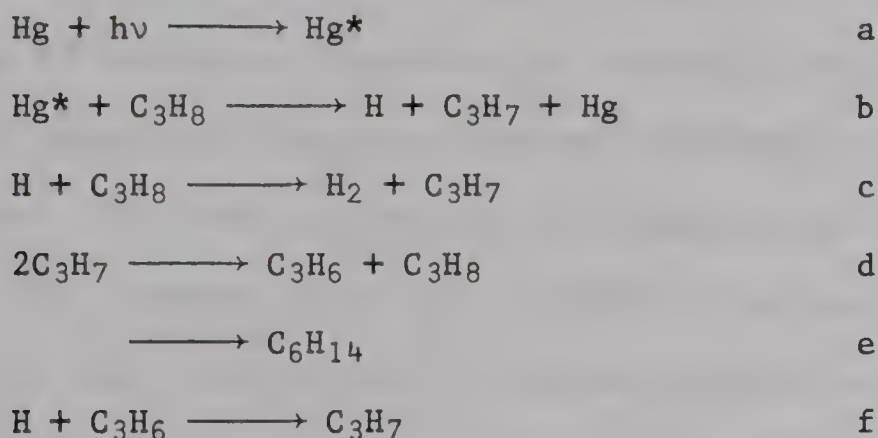


Fig. 2 The photolytic assembly



region above 3150 Å. For the H-atom system the source was a Hanovia 2537 Å low pressure mercury arc equipped with a Vycor 7910 filter to eliminate wavelengths below 2200 Å.

For the H-atom + ethylene episulfide system lamp intensities were determined using propane actinometry. Under conditions of low lamp intensities the primary processes are:



where  $\text{Hg}^* = \text{Hg}(^3\text{P}_1)$  and  $\text{Hg} = \text{Hg}(^1\text{S}_0)$ . Although *n*- and *iso*- $\text{C}_3\text{H}_7$  radicals are produced they need not be differentiated here. Back<sup>47</sup> has shown that  $\phi(\text{H}_2)$ , the quantum yield of hydrogen production, decreases with irradiation time until the concentration of  $\text{C}_3\text{H}_6$  reaches a steady state, after which  $\phi(\text{H}_2) = 0.58$  and remains constant<sup>48</sup>. Experimentally, about 700 torr propane was irradiated repeatedly until the rate of hydrogen production was constant and this was then used to calculate the lamp intensity. The lamp intensity was kept low, of the order of  $3 \times 10^{14}$  photons  $\text{sec}^{-1}$ , in order to minimize radical-radical reactions and the concentration of H-atoms.



#### 4. Materials

Most of the chemicals used were of research grade and were purified by distillation *in vacuo*. Table IV lists the sources and methods of purification of the various compounds used in this study.

Propylene and 2-butene episulfides were prepared from the cyclic carbonate ester by the method of Searles and Lutz<sup>49</sup>. Equimolar amounts of respective carbonate and potassium thiocyanate (BDH) were gently heated and the episulfide was continuously distilled out of the mixture. The crude product was then degassed and distilled *in vacuo* at  $\sim 1$  torr pressure, with only the middle fraction being retained. The *cis*- and *trans*-isomers of 2-butene episulfide were separated by g.c. on a 7 ft. tricresylphosphate column (20% on Chromosorb W) at 80°C and a flow rate of 150 cc/min ( $t_R$  *trans* = 15 min, *cis* = 21 min). The purified episulfides were always stored *in vacuo* at -196°C.

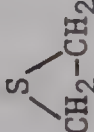
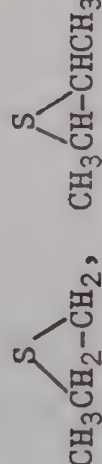
Propylene carbonate was commercially available (Eastman Organic). The carbonate ester of 2,3-butanediol was prepared<sup>50</sup> by refluxing a mixture of 2,3-butanediol (1 mole), diethyl carbonate (1.1 mole) and a small cube of sodium catalyst for three hours. The alcohol product was distilled out of the mixture and the remaining fraction was dissolved in benzene, washed in a small quantity of water then dried over calcium chloride. After removal of benzene, the crude product was distilled at reduced pressure (150  $\mu$ /65-76°) and the middle portion recrystallized from ether.





TABLE IV

## Sources of Materials and Purification Procedures

Material	Source	Purification
$C_2H_6$ , $C_2H_4$ , $C_3H_6$ ,	Phillips, 99.5% pure	degassed at $-196^\circ C$
2 - $C_4H_8$	"	"
$H_2$	Matheson 99.9995% pure	used as such
$N_2$	Airco research grade	used as such
$H_2S$	Matheson	distilled at $-130^\circ C$
	Pierce chemicals	distilled at $-161^\circ C$
$CH_3N = NCH_3$	Merck	degassed at $-130^\circ C$ distilled at $-98^\circ C$
	lab. prepared	see text
$CH_3SCH_3$ , $CH_3SSCH_3$	Matheson, Coleman and Bell	used as such



## 5. Analytical Techniques

The analytical system, illustrated in Figure 3, consisted of a calibrated gas burette connected to the injection loop of a gas chromatograph. The gas chromatograph consisted of a hot wire detector (GowMac Model TR II B) and a power supply unit (GowMac Model 9999C). The signals were recorded on a Sargent recorder, Model S-72180. Helium, dried and purified by passing through an Ascarite-Drierite mixture, was used as a carrier gas, at flow rates determined by an oil manometer calibrated by a soap bubble flow meter. The types of g.c. columns used, the operating conditions and retention times of the various compounds encountered in this work are summarized in Table V.

The g.c. effluent could be passed through a series of traps in which the desired compounds could be isolated for purpose of analysis. Product identifications were made by comparing the g.c. retention time and mass spectra with those of authentic materials. The detector response was calibrated from authentic samples and checked periodically for reproducibility. Peak areas were measured with an Otto planimeter.

## 6. Operational Procedure

The reaction cell was heated overnight to the desired temperature and the lamp was allowed to equilibrate at least 30 minutes prior to irradiation. Control experiments were made at each





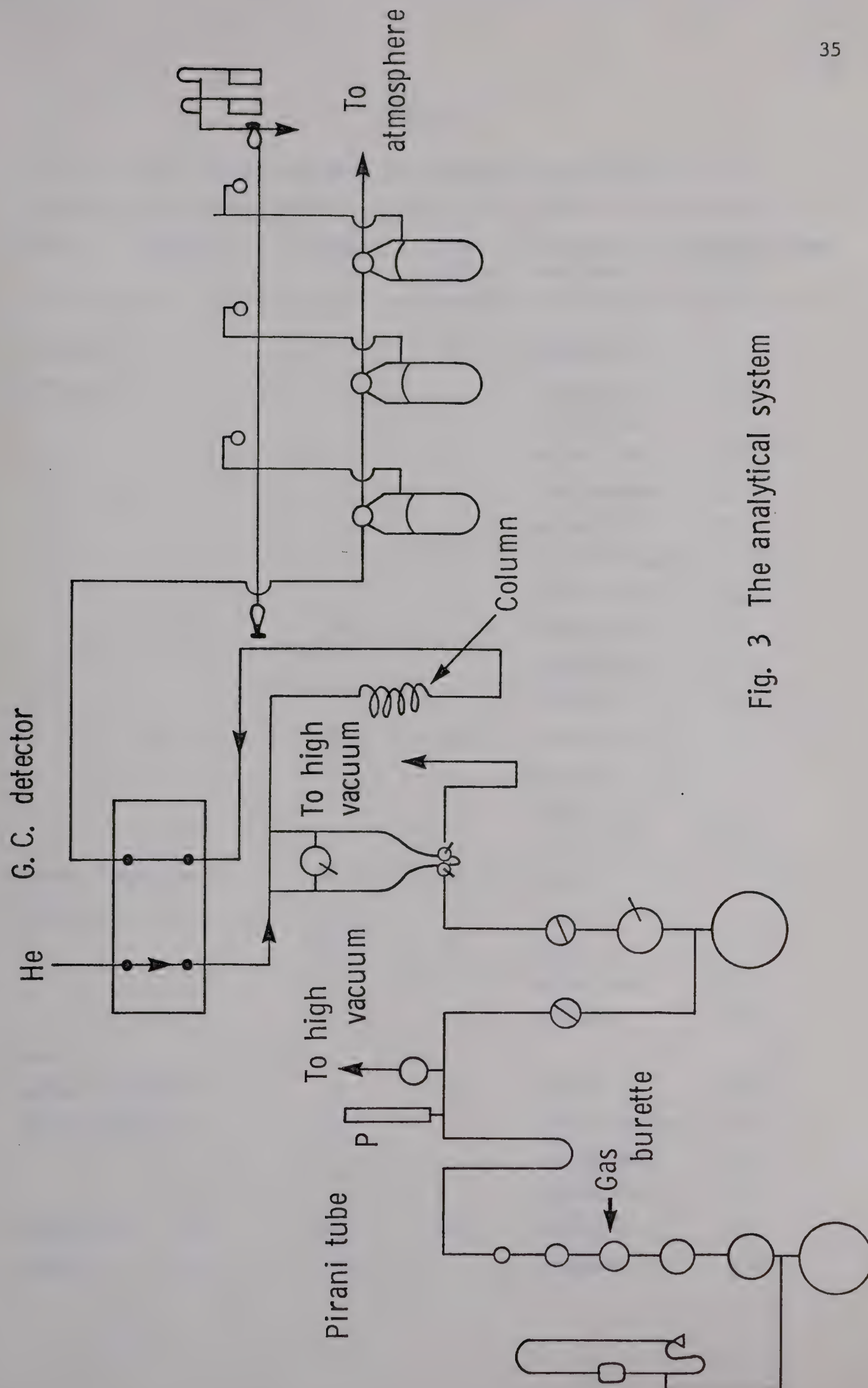


Fig. 3 The analytical system



TABLE V

## G.C. Retention Data and Operating Conditions

Column	Length, ft.	Temp. °C	Flow cc/min.	Compounds analyzed	Retention time min.
Tricresyl phosphate	5	52	60	ethylene	
				episulfide	7.2
				propylene	
				episulfide	8.3
				<i>cis</i> -butene	
				episulfide	25.5
				<i>trans</i> -butene	
				episulfide	16.5
				azomethane	3.1
				C <sub>2</sub> H <sub>5</sub> N=N-CH <sub>3</sub>	5.7
				CH <sub>3</sub> CH <sub>2</sub> SH	3.3
"	16	80	60	dimethyl	
				sulfide	6
				dimethyl	
				disulfide	35
Medium activity 15 silica gel	15	88	60	C <sub>2</sub> H <sub>4</sub>	5.2
		108	80	H <sub>2</sub> S	15.2
				propylene	11.2
				ethane	2.1
Diethyl adipate (15%) on chromosorb W	20	0	45	ethane	2.8
				<i>trans</i> -butene	10.1
				<i>cis</i> -butene	11.5
				azomethane	16.1
Molecular Sieve	10	25	60	nitrogen	2.8
				methane	4.5



temperature in order to correct for the amount of olefin produced by thermal decomposition of the episulfide.

#### (a) Methyl Radical Reactions

Azomethane and episulfide were purified by trap-to-trap distillation prior to each experiment and measured quantities were admitted to the cell at low pressure in order to avoid contamination by mercury vapour. The mixture was allowed to equilibrate for 20 minutes, then irradiated. Non-condensable gases were analyzed on a molecular sieve column. For the  $\text{CH}_3$  + propylene episulfide system, the fraction volatile at  $-130^\circ\text{C}$  was analyzed on a medium activity silica gel column. Azomethane and propylene episulfide were then recovered at  $-98^\circ\text{C}$  and the remaining condensable fraction, consisting of methyl sulfide, dimethyl sulfide, and methyl ethyl diimide, was resolved on a tricresyl phosphate column. In the  $\text{CH}_3$  + 2-butene episulfide reaction, the fraction volatile at  $-130^\circ\text{C}$  (*cis*- and *trans*-2-butene, ethane) was analyzed on a diethyl adipate column. Azomethane and butene episulfide were then separated at  $-98^\circ\text{C}$  and  $-78^\circ\text{C}$  respectively.

#### (b) Hydrogen Atom Reactions

The photolysis assembly was heated overnight to the desired temperature and the lamp was allowed to equilibrate 30 minutes. Measured amounts of ethylene episulfide and  $\text{H}_2\text{S}$  were condensed into





the cell then about 500 torr  $H_2$  was introduced. The circulating pump was then turned on and the mixture was equilibrated 30 minutes. After photolysis,  $H_2$  was pumped out very slowly through a series of traps at  $-196^\circ C$  and  $-212^\circ C$ . The fraction volatile at  $-160^\circ C$ , consisting of  $C_2H_4$  and traces of  $H_2S$ , was analyzed on a silica gel column. In the experiments with added  $H_2S$ ,  $H_2S$  was removed at  $-130^\circ C$  and ethylene episulfide at  $-98^\circ C$ .



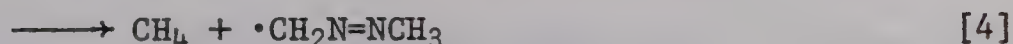
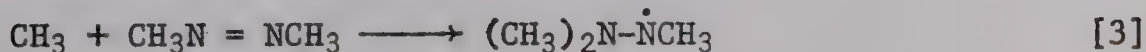
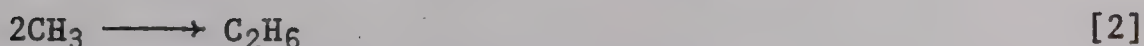
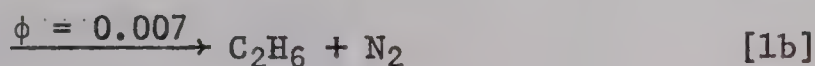
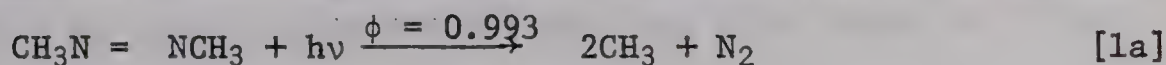
## CHAPTER III

## RESULTS

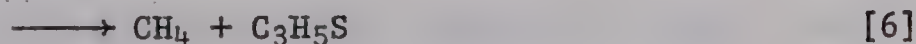
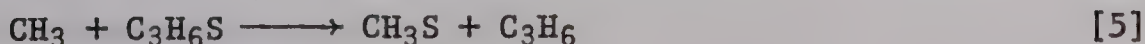
## 1. Methyl Radical Reactions

## (a) With Propylene Episulfide

The photolysis of azomethane in the presence of propylene episulfide (PES) gave rise to the formation of  $N_2$ ,  $CH_4$ ,  $C_2H_6$ ,  $C_3H_6$ ,  $CH_3SCH_3$ ,  $CH_3SSCH_3$ , methyl ethyl diimide and polymer. The nature of the products and their relative yields can be rationalized in terms of the elementary reactions occurring in the photolysis of azomethane<sup>43,44</sup>,



the competing reactions with PES,



and secondary reactions involving methyl thiyl radicals:

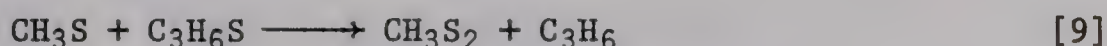








Owing to the low vapour pressure of PES, the product yields were necessarily small. Hence the fate of the  $\text{C}_3\text{H}_5\text{S}$  radical could not be determined in this system but since no retrievable products arising from this radical were detected, it probably ends up as polymer. Similarly, corrections to the  $\text{C}_3\text{H}_6$  yields for the abstraction reaction by  $\text{CH}_3\text{S}$  radicals,



could not be estimated. However, the  $\text{C}_3\text{H}_6/2\text{N}_2$  ratio did not increase significantly with temperature and it seems therefore that reaction [9] is not as important as in the  $\text{CH}_3$  + ethylene episulfide system.

The rates of formation of the major products as a function of temperature in the range 66–162°C are listed in Table VI. Since  $R_{\text{C}_3\text{H}_6}$  is related to  $R_{\text{C}_2\text{H}_6}$  via the relation

$$[\text{PES}]^{-1} \left( R_{\text{C}_3\text{H}_6} / R_{\text{C}_2\text{H}_6}^{1/2} \right) = k_5 / k_2^{1/2}$$

and since  $\log k_2 = 13.34^{+2}$  the rate parameters for reaction [5], calculated from a least mean squares analysis of the Arrhenius plot shown in Figure 4 are:

$$\log k_5 = 11.33 \pm 0.92 - (7450 \pm 1660/RT) (\text{cc mole}^{-1} \text{ sec}^{-1})$$

Also, the rate equation for  $\text{CH}_4$  production is given by:

$$k_6 / k_2^{1/2} = \left( R_{\text{CH}_4} / R_{\text{C}_2\text{H}_6}^{1/2} - k_4 / k_2^{1/2} [\text{azo}] \right) [\text{PES}]^{-1}$$



TABLE VI

## Reactions of Methyl Radicals with Propylene Episulfide

Rates of Product Formation as a Function of Temperature<sup>a</sup>

Temp °C	[PES] x 10 <sup>6</sup> mole/cc	[(CH <sub>3</sub> N) <sub>2</sub> ]	Rates of formation x 10 <sup>13</sup> mole/cc sec.				$k_5/k_2^{1/2}$	$k_6/k_2^{1/2}$ x 10
			N <sub>2</sub>	C <sub>2</sub> H <sub>6</sub>	CH <sub>4</sub>	C <sub>3</sub> H <sub>6</sub>		
66	1.83	0.35	42.71	19.81	3.14	19.88	7.80	0.94
87	1.67	0.52	73.69	19.55	8.11	26.72	11.42	2.47
110	1.61	0.45	71.43	11.15	14.23	54.81	32.11	-
129	1.75	0.51	82.58	5.57	14.21	60.55	46.48	7.83
135	1.80	0.35	59.15	3.55	11.49	53.97	50.18	8.42
138	1.76	0.47	66.89	4.08	14.72	37.14	33.03	9.75
153	1.74	0.41	42.52	2.79	13.55	54.05	58.88	10.68
162	5.77	1.18	32.48	7.00	100.72	522.41	108.40	16.18

<sup>a</sup> Photolysis time, 45 min., cell volume = 190 cc.



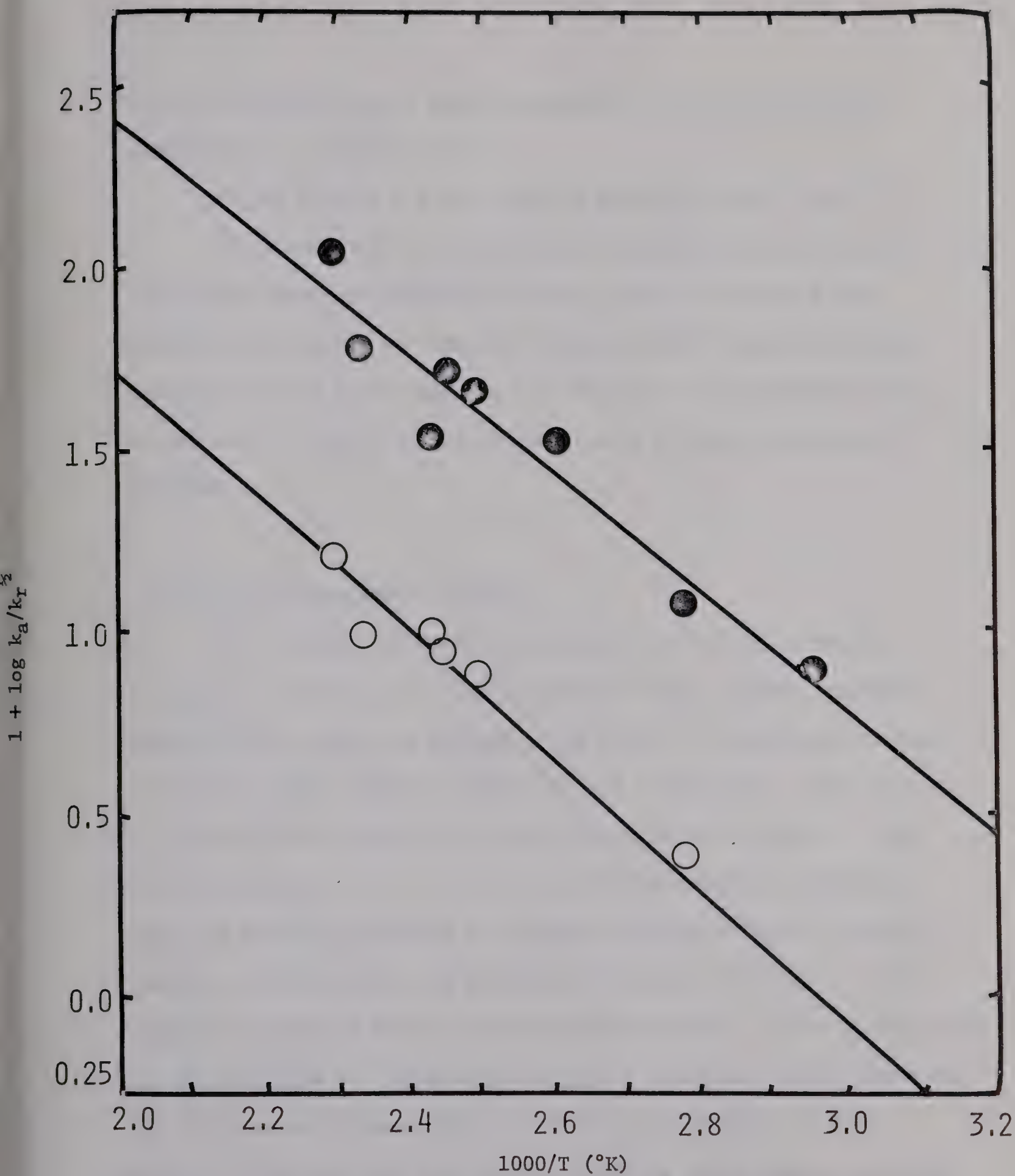


Figure 4. Arrhenius Plot for S-Abstraction (●) and H-Abstraction (○) from Propylene Episulfide by Methyl Radicals





From the Arrhenius plot, also illustrated in Figure 4, the rate parameters for reaction 6 are:

$$\log k_6 = 11.00 \pm 0.48 - (8260 \pm 870/RT)(\text{cc mole}^{-1} \text{ sec}^{-1}).$$

The possibility of an additional  $\text{CH}_4$  producing reaction via the radical disproportionation step  $\text{CH}_3 + \text{CH}_3\text{S} \longrightarrow \text{CH}_4 + \text{CH}_2\text{S}$  cannot be discounted but there is some evidence<sup>51</sup> that the rate of this reaction is small compared with the rate of recombination, [7]. In any case, it would not be expected to be strongly temperature dependent.

(b) With *cis*-2-Butene Episulfide

The reactions of methyl radicals with *cis*-2- $\text{C}_4\text{H}_8\text{S}$  (BES) produce  $\text{N}_2$ ,  $\text{CH}_4$ ,  $\text{C}_2\text{H}_6$ , *cis*-2- $\text{C}_4\text{H}_8$ , *trans*-2- $\text{C}_4\text{H}_8$ ,  $\text{CH}_3\text{SCH}_3$ ,  $\text{CH}_3\text{SSCH}_3$ , methyl ethyl diimide and polymer. The effect of irradiation time on the major product yields at 118°C is seen in Table VII. The *cis*-2- $\text{C}_4\text{H}_8$ /*trans*-2- $\text{C}_4\text{H}_8$  ratios are plotted versus time in Figure 5. The marked decrease in the ratio with increasing conversion indicates that the initially produced *cis* olefin undergoes efficient isomerization to the *trans* form via secondary reactions, of which the most important is methyl radical catalyzed isomerization. This is supported by the fact that a 30 minute photolysis of azomethane in the presence of *cis*-2-butene produced large yields of *trans*-2-butene. From Figure 5 it is seen that the initial yield of *cis*-2-butene is about 80%, indicating a very high degree of stereoselectivity in the



TABLE VII

Effect of Conversion on the Product Yields from the Reactions of Methyl Radicals with *cis*-2-Butene Episulfide<sup>a</sup>

Time, min.	[BES] <sup>b</sup> x 10 <sup>6</sup> mole/cc	Rates, x 10 <sup>9</sup> mole/cc sec					<i>cis</i> -2-C <sub>4</sub> H <sub>8</sub>
		[ (CH <sub>3</sub> N) <sub>2</sub> ]				<i>trans</i> -2-C <sub>4</sub> H <sub>8</sub>	
		N <sub>2</sub>	C <sub>2</sub> H <sub>6</sub>	CH <sub>4</sub>	<i>cis</i> -2-C <sub>4</sub> H <sub>8</sub>		
5	1.36	0.85	1.85	-	1.33	0.42	3.19
15	1.68	1.09	0.23	0.20	2.42	0.94	2.57
30	1.45	3.50	0.10	0.17	2.83	0.98	2.89
45	1.54	1.17	0.32	0.07	1.33	1.03	1.29

<sup>a</sup> T = 118°C ;

<sup>b</sup> BES = *cis*-2-butene episulfide



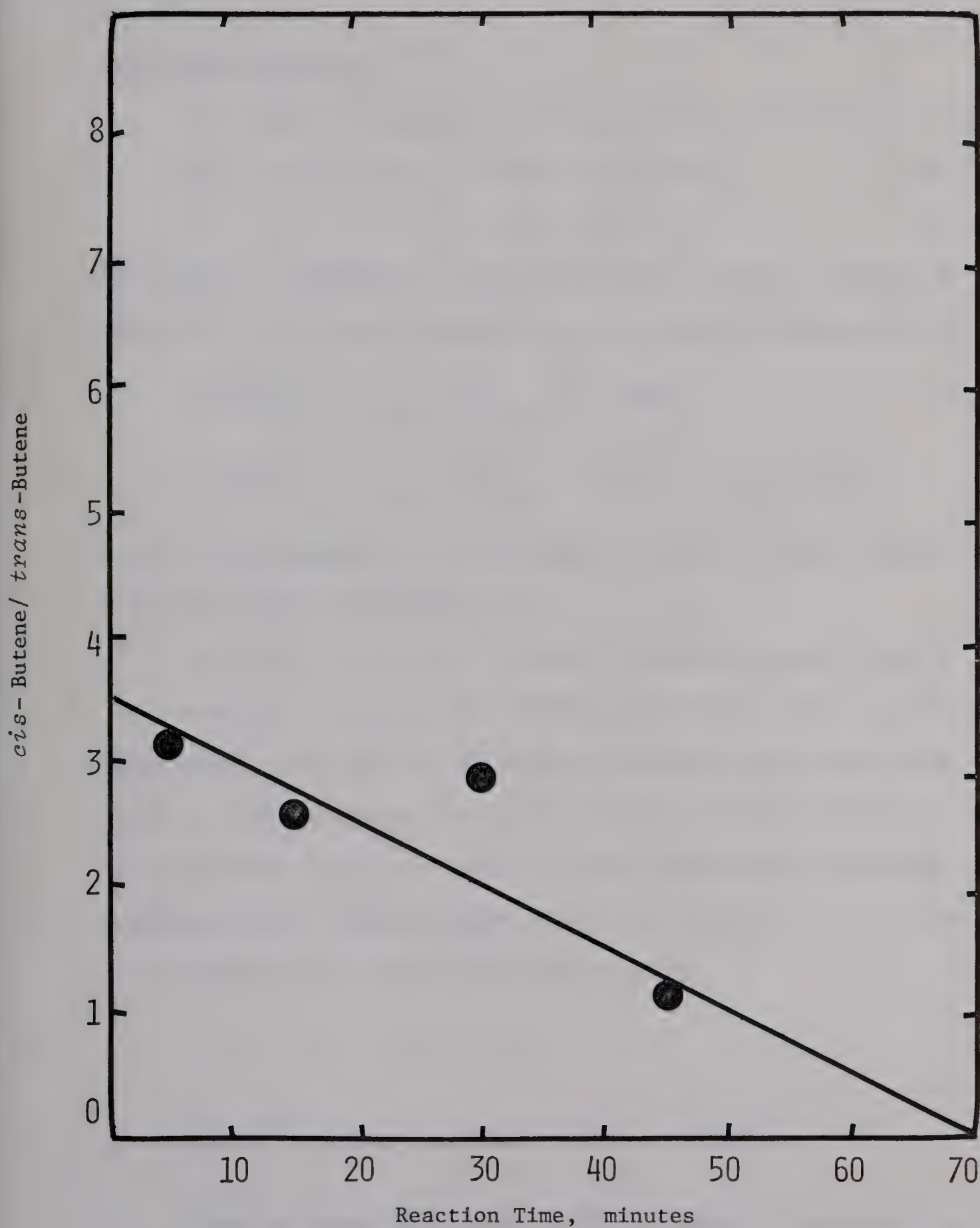


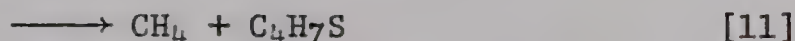
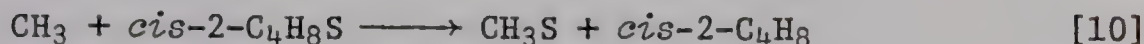
Figure 5. Effect of Reaction Time on the *cis*-Butene/*trans*-Butene Ratio from the Reaction of Methyl Radicals with *cis*-2-Butene Episulfide.





abstraction reaction.

The reaction sequence follows steps [1] - [4], [7], [8] and



The effect of temperature on the major product yields is listed in Table VIII. The kinetic expressions for S- and H- abstraction are,

$$k_{10}/k_2^{\frac{1}{2}} = \left( R_{\text{C}_4\text{H}_8} / R_{\text{C}_2\text{H}_6}^{\frac{1}{2}} \right) [\text{BES}]^{-1}$$

$$k_{11}/k_2^{\frac{1}{2}} = \left( R_{\text{CH}_4} / R_{\text{C}_2\text{H}_6}^{\frac{1}{2}} - k_4/k_2^{\frac{1}{2}} [\text{azo}] \right) [\text{BES}]^{-1}$$

and the rate parameters for reactions [10] and [11] were obtained from the Arrhenius plot, Figure 6:

$$\log k_{10} = 12.31 \pm 2.57 - (6800 \pm 3900/RT)(\text{cc mole}^{-1} \text{ sec}^{-1})$$

$$\log k_{11} = 11.03 \pm 1.52 - (7000 \pm 2410/RT)(\text{cc mole}^{-1} \text{ sec}^{-1})$$

Since most, if not all, of the *trans*-2-butene product arises from methyl radical isomerization of the initially formed *cis*-2-butene and the experiments listed in Table VIII were performed at relatively large conversions, the combined yields of *cis* and *trans* olefin were used in the calculation of the rate constant ratios.

## 2. Hydrogen Atom Reactions With Ethylene Episulfide

Hydrogen atoms were generated by the mercury photosensitization of  $\text{H}_2^{52}$ :



TABLE VIII

Effect of Temperature on the Product Yields from the Reactions of Methyl Radicals with *cis*-2-Butene Episulfide<sup>a</sup>

Temp °C	[BES] <sup>b</sup> x 10 <sup>6</sup> mole/cc	[(CH <sub>3</sub> N) <sub>2</sub> ]	Rates x 10 <sup>9</sup> mole/cc sec.				log k <sub>10</sub> /k <sub>2</sub> <sup>1/2</sup>	log k <sub>11</sub> /k <sub>2</sub> <sup>1/2</sup>
			N <sub>2</sub>	C <sub>2</sub> H <sub>6</sub>	CH <sub>4</sub>	<i>cis</i> -2-C <sub>4</sub> H <sub>8</sub>	<i>trans</i> -2-C <sub>4</sub> H <sub>8</sub>	
121	1.16	0.21	2.89	0.70	0.83	1.97	1.24	2.07
100	0.79	0.20	3.36	1.73	0.19	0.68	0.67	1.61
94	1.11	0.24	3.45	1.69	0.55	1.27	0.86	1.74
72	1.34	0.24	2.69	1.77	0.18	0.51	0.29	1.87
53	1.19	0.21	2.76	2.03	0.08	0.29	0.19	0.96
30	1.05	0.20	2.43	2.07	0.06	0.23	0.11	0.85

<sup>a</sup> Photolysis time, 45 minutes;

<sup>b</sup> BES = *cis*-2-butene episulfide; cell volume = 190 cc



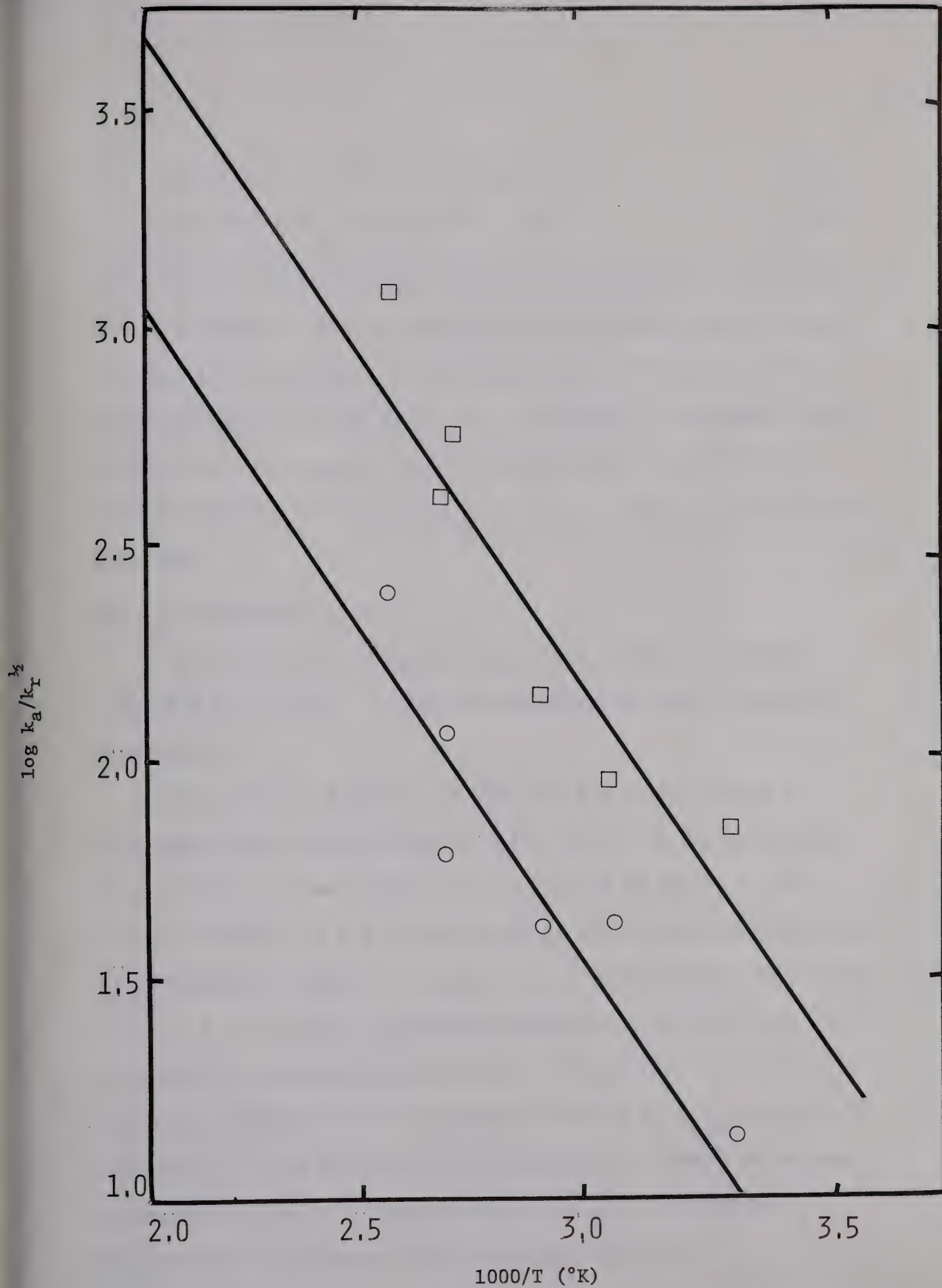
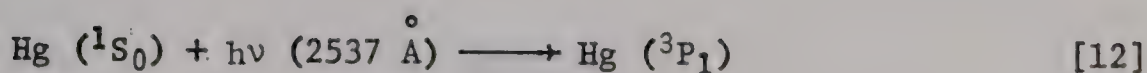


Figure 6. Arrhenius Plot for S-Abstraction ( $\square$ ) and H-Abstraction ( $\circ$ ) from *cis*-2-Butene Episulfide by Methyl Radicals







The extinction coefficient of ethylene sulfide (EES) at 2537  $\text{\AA}$  is small, compared to that of mercury, and its concentration was kept very low (of the order of 5 torr), therefore it is unlikely that direct photolysis of EES could occur. Similarly, photosensitization of EES cannot be important since the quenching cross-section is smaller than that of  $\text{H}_2$  and the ratio of  $\text{H}_2$  to EES was always greater than 100.

(a) In the Absence of  $\text{H}_2\text{S}$

The only products observed from the  $\text{H} + \text{EES}$  reaction were  $\text{C}_2\text{H}_4$ ,  $\text{H}_2\text{S}$  and polymer.  $\text{C}_2\text{H}_5\text{SH}$  was demonstrably absent, under all conditions.

The rates of formation of  $\text{C}_2\text{H}_4$  and  $\text{H}_2\text{S}$  produced from the room temperature sensitization of  $\sim 500$  torr  $\text{H}_2$  in the presence of 5 torr EES are listed in Table IX and plotted in Figure 7. The rate of formation of  $\text{H}_2\text{S}$  is unaffected by increasing conversion, but  $R_{\text{C}_2\text{H}_4}$  appears to decline. In order to ascertain whether this effect is real, i.e. a result of secondary reactions, quantum yields were determined at various exposure times. The results, listed in Table X, demonstrate that the apparent decline in  $R_{\text{C}_2\text{H}_4}$  is due to attenuation of the incident light intensity as a result of polymer deposition on the cell face and that the rates of formation of  $\text{C}_2\text{H}_4$  and  $\text{H}_2\text{S}$  are constant with increasing conversion.



TABLE IX

Reactions of Hydrogen Atoms with Ethylene Episulfide. Effect of Exposure Time on the Product Yields<sup>a</sup>

Time Minutes	Rates x 10 <sup>8</sup> mole/min	
	C <sub>2</sub> H <sub>4</sub>	H <sub>2</sub> S
15	7.93	1.23
30	7.79	1.24
45	7.64	1.25
60	7.49	1.26
90	7.20	1.27

<sup>a</sup> P<sub>H<sub>2</sub></sub> = 500 torr

P<sub>EES</sub> = 5 torr

T = 27°C



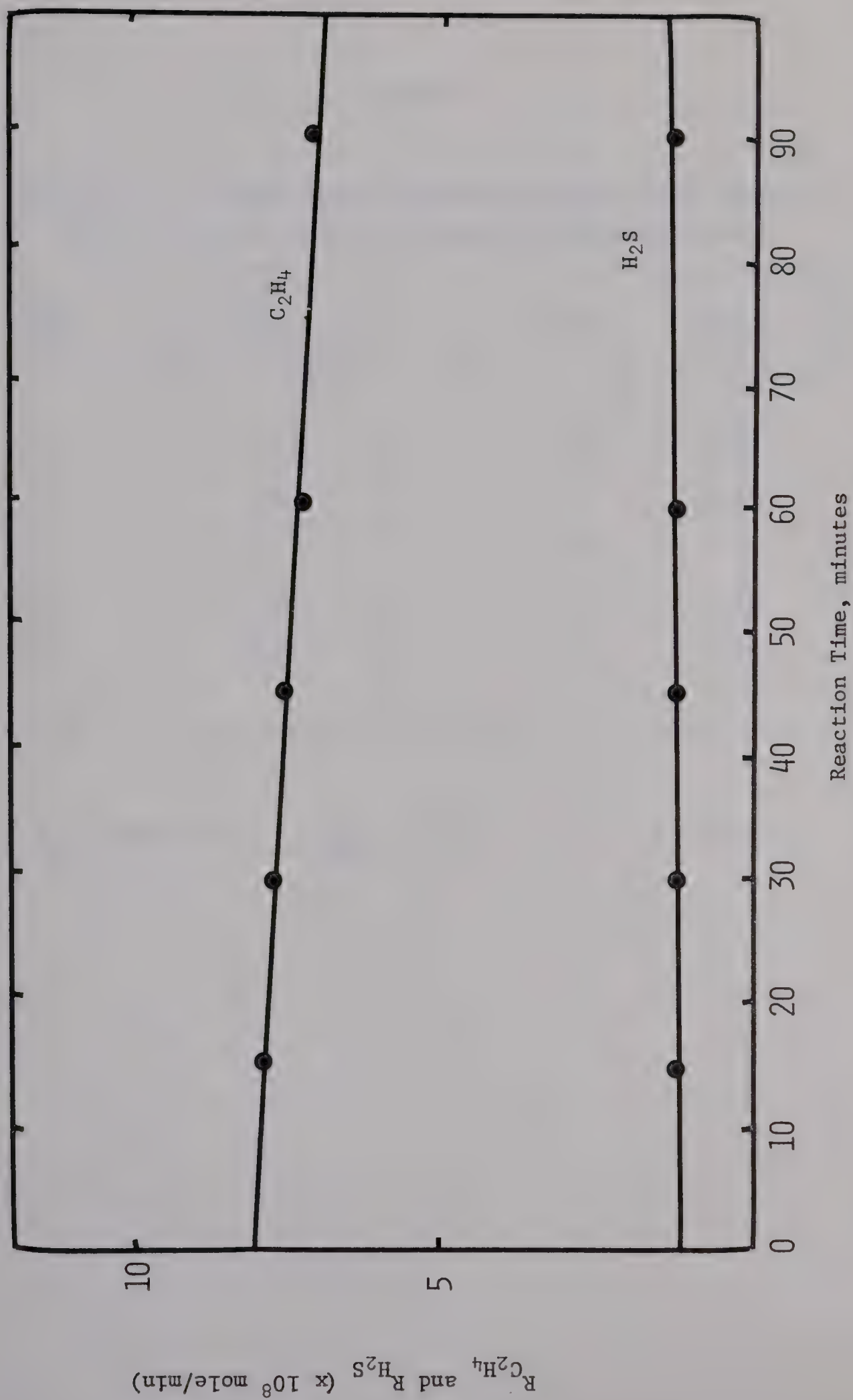


Figure 7. Effect of Exposure Time on the Product Yields of the H-Atom Reaction with Ethylene Episulfide





TABLE X

Reactions of Hydrogen Atoms with Ethylene Episulfide. Quantum Yields of  $\text{H}_2\text{S}$  and  $\text{C}_2\text{H}_4$  as a Function of Exposure Time.

Time, min.	$I_a$ $\times 10^8$ Einstein/min.	$\phi_{\text{C}_2\text{H}_4}$	$\phi_{\text{H}_2\text{S}}$
15	3.19	2.49	0.39
30	3.15	2.47	0.39
45	3.11	2.46	0.40
60	3.07	2.44	0.41
90	2.98	2.42	0.42

<sup>a</sup>  $P_{\text{H}_2} = 500$  torr,  $P_{\text{EES}} = 5$  torr  $T = 27^\circ\text{C}$



The effect of EES concentration on the product yields was also examined, and the results are given in Table XI. It is clear that  $R_{C_2H_4}$  and  $R_{H_2S}$  are unaffected by the episulfide pressure.

Quantum yields of formation of  $C_2H_4$  and  $H_2S$  were also measured at 96 and 152°C. The results are summarized in Table XII.

Since ethylene is a major product it appears that the major primary process in the  $H + EES$  reaction is sulfur abstraction:

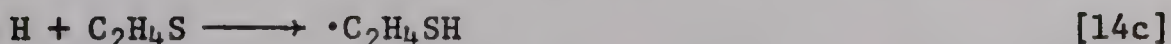


Direct evidence for hydrogen abstraction,



is lacking since the  $C_2H_3S$  radical, if formed, does not lead to retrievable products. Kinetic treatment of the data, however, points to step [14a] as the only observable process.

The possibility of addition of H-atoms to the sulfur moiety,



is conceptually uninviting and in fact,  $C_2H_5SH$  was not detected.

$H_2S$  is not likely to be formed via abstraction by the  $HS$  radical from either  $H_2$  or  $EES$ , since the C-H bond energies in these compounds are substantially higher than the H-S bond energy in  $H_2S$  and the activation energies for these processes must consequently be very large. The only viable route is disproportionation of  $HS$  radicals:





TABLE XI

Reactions of Hydrogen Atoms with Ethylene Episulfide. Rates of Formation of  $C_2H_4$  and  $H_2S$  as a Function of Episulfide Pressure.<sup>a</sup>

P(EES), torr	Rates, $\times 10^8$ mole/min	
	$C_2H_4$	$H_2S$
1.00	7.05	1.22
2.15	8.13	1.38
2.01	7.28	1.27
3.03	7.47	1.34
5.20	7.65	1.01
5.09	7.13	1.19
4.81	8.03	-
5.32	7.60	1.30
7.22	7.82	1.27

<sup>a</sup>  $P(H_2) = 490$  torr,  $T = 27^\circ C$ , exposure time = 60 minutes





TABLE XII

Quantum Yields of  $C_2H_4$  and  $H_2S$  as a Function of Temperature<sup>a</sup>

Temp, °C	$\phi_{C_2H_4}$	$\phi_{H_2S}$
27	$2.46 \pm 0.02$	$0.40 \pm 0.01$
96	$2.39 \pm 0.07$	$0.39 \pm 0.01$
152	$2.23 \pm 0.03$	$0.19 \pm 0.03$

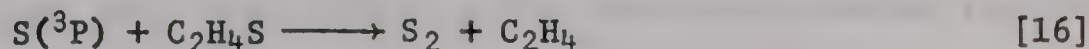
<sup>a</sup>  $P(H_2) = 490$  torr,  $P(EES) = 5$  torr, exposure time, 60 minutes



Other bimolecular reactions involving the HS radicals are:



The combination and disproportionation reactions of HS radicals are not well understood although they have been extensively studied<sup>54-58</sup>. Although there is unequivocal experimental evidence for the occurrence of steps [15a] - [15d], the relative rates of each process are not known. It appears, however, that step [15a] is of major importance and since this step produces sulfur atoms the following reaction must be included in the sequence



Kinetic analysis of the reaction sequence [12] - [16] leads to the following steady-state concentrations:

$$[\text{H}] = \frac{2 I_a}{k_{14} [\text{EES}]}$$

$$[\text{HS}]^2 = \frac{k_{14a} I_a}{k_{14} k_{15}} \quad \text{where } k_{14} = k_{14a} + k_{14b} \quad \text{and } k_{15} = k_{15a} + k_{15b} + k_{15c} + k_{15d}$$

$$[\text{S}] = \frac{k_{14a} k_{15a} I_a}{k_{14} k_{15} k_{16} [\text{EES}]}$$

The quantum yields of formation of  $\text{C}_2\text{H}_4$  and  $\text{H}_2\text{S}$  are:

$$\phi_{\text{C}_2\text{H}_4} = \frac{2k_{14a}}{k_{14}} \left( 1 + \frac{k_{15a}}{2k_{15}} \right)$$



$$\phi_{\text{H}_2\text{S}} = \frac{k_{14a} \cdot k_{15a}}{k_{14} \cdot k_{15}}$$

from which

$$\phi_{\text{C}_2\text{H}_4} - \phi_{\text{H}_2\text{S}} = 2 \frac{k_{14a}}{k_{14}}$$

and

$$\phi_{\text{C}_2\text{H}_4} / \phi_{\text{H}_2\text{S}} = 2 \frac{k_{15}}{k_{15a}} + 1$$

Values of  $\phi_{\text{C}_2\text{H}_4} - \phi_{\text{H}_2\text{S}}$  and  $k_{15a}/k_{15}$  are listed in Table XIII at 27, 96 and 152°C. Since  $\phi_{\text{C}_2\text{H}_4} - \phi_{\text{H}_2\text{S}}$  is constant and equal to 2 within experimental error, it can be concluded that sulfur abstraction, step [14a], is the only primary process in the H + EES system. It is also seen from Table XIII that the disproportionation reaction of HS radicals to yield  $\text{H}_2\text{S} + \text{S}$ , step [15a], is the major mode of removal of HS radicals at room temperature, but diminishes in importance with increasing temperature.

(b) In the Presence of  $\text{H}_2\text{S}$

When  $\text{H}_2\text{S}$  is added to the system, H-atom abstraction,



will compete with S-atom abstraction, [14]. The concentrations of  $\text{H}_2\text{S}$  were always very small in order to minimize direct photolysis or sensitization.

The effect of  $\text{H}_2\text{S}$  pressure on  $\phi_{\text{C}_2\text{H}_4}$  at 27, 96 and 152°C





TABLE XIII

$\phi_{\text{C}_2\text{H}_4} - \phi_{\text{H}_2\text{S}}$  and  $k_{15a}/k_{15}$  from the  
H + EES Reaction

Temp, °C	$\phi_{\text{C}_2\text{H}_4} - \phi_{\text{H}_2\text{S}}$	$k_{15a}/k_{15}$
27	2.02	0.41
96	2.00	0.39
152	2.04	0.19



are listed in Table XIV. Analysis of the kinetic sequence [12] - [17] leads to the following expression for the quantum yield of ethylene production:

$$\phi_{\text{C}_2\text{H}_4} = \frac{2}{1 + \frac{k_{17}[\text{H}_2\text{S}]}{k_{14}[\text{EES}]}} + \frac{k_{15a}}{k_{15}}$$

from which

$$\gamma = (\phi_{\text{C}_2\text{H}_4} - k_{15a}/k_{15})^{-1} = \frac{1}{2} + \frac{k_{17}[\text{H}_2\text{S}]}{k_{14}[\text{EES}]}$$

Values of  $\gamma$  are also listed in Table XIV and are plotted as a function of  $[\text{H}_2\text{S}]/[\text{EES}]$  in Figure 8. Least mean squares analyses of these plots yield the slope and intercept values listed in Table XV. The errors are quoted in terms of standard deviations and are obviously much too small since the difficulties encountered in the analyses of  $\text{H}_2\text{S}$  lead to considerable uncertainties in the calculated values of  $k_{15a}/k_{15}$ . Also, the contribution to the overall  $\text{C}_2\text{H}_4$  yield from step [16] will be more important in this system owing to a high concentration of HS radicals. The calculated intercepts therefore are probably close enough to the theoretical value of 0.5 to justify the overall kinetic treatment of the data.

The Arrhenius plot of  $\log k_{17}/k_{14}$  versus temperature is illustrated in Figure 9, from which

$$E_{14} - E_{17} = 235 \pm 115 \text{ cal mole}^{-1}$$

and  $A_{14}/A_{17} = 7.3 \pm 1.2$



TABLE XIV

Effect of  $\text{H}_2\text{S}$  Pressure on  $\phi_{\text{C}_2\text{H}_4}$  in the  $\text{H} + \text{EES} + \text{H}_2\text{S}$  System<sup>a</sup>

Temp., °C	Pressure, torr		$\phi_{\text{C}_2\text{H}_4}$	$\gamma$
	$\text{H}_2\text{S}$	EES		
27	4.33	1.05	2.36	0.513
	3.02	1.02	2.40	0.503
	4.89	4.89	2.21	0.556
	3.00	3.02	2.09	0.595
	2.89	5.63	1.87	0.685
	3.05	5.97	1.90	0.671
96	3.07	0.998	2.36	0.508
	2.97	2.89	2.05	0.602
	3.02	3.07	2.17	0.562
	3.00	3.10	2.10	0.585
	3.00	5.97	1.85	0.685
	2.77	5.91	1.88	0.671
152	3.10	0.95	2.16	0.508
	2.94	0.97	2.08	0.529
	2.41	0.88	2.14	0.513
	3.43	3.00	2.02	0.546
	3.02	3.00	1.85	0.602
	3.00	3.20	1.95	0.568
	3.05	5.86	1.70	0.662
	3.02	5.99	1.72	0.654
	2.89	5.89	1.67	0.676

<sup>a</sup>  $P_{\text{H}_2} = 490$  torr





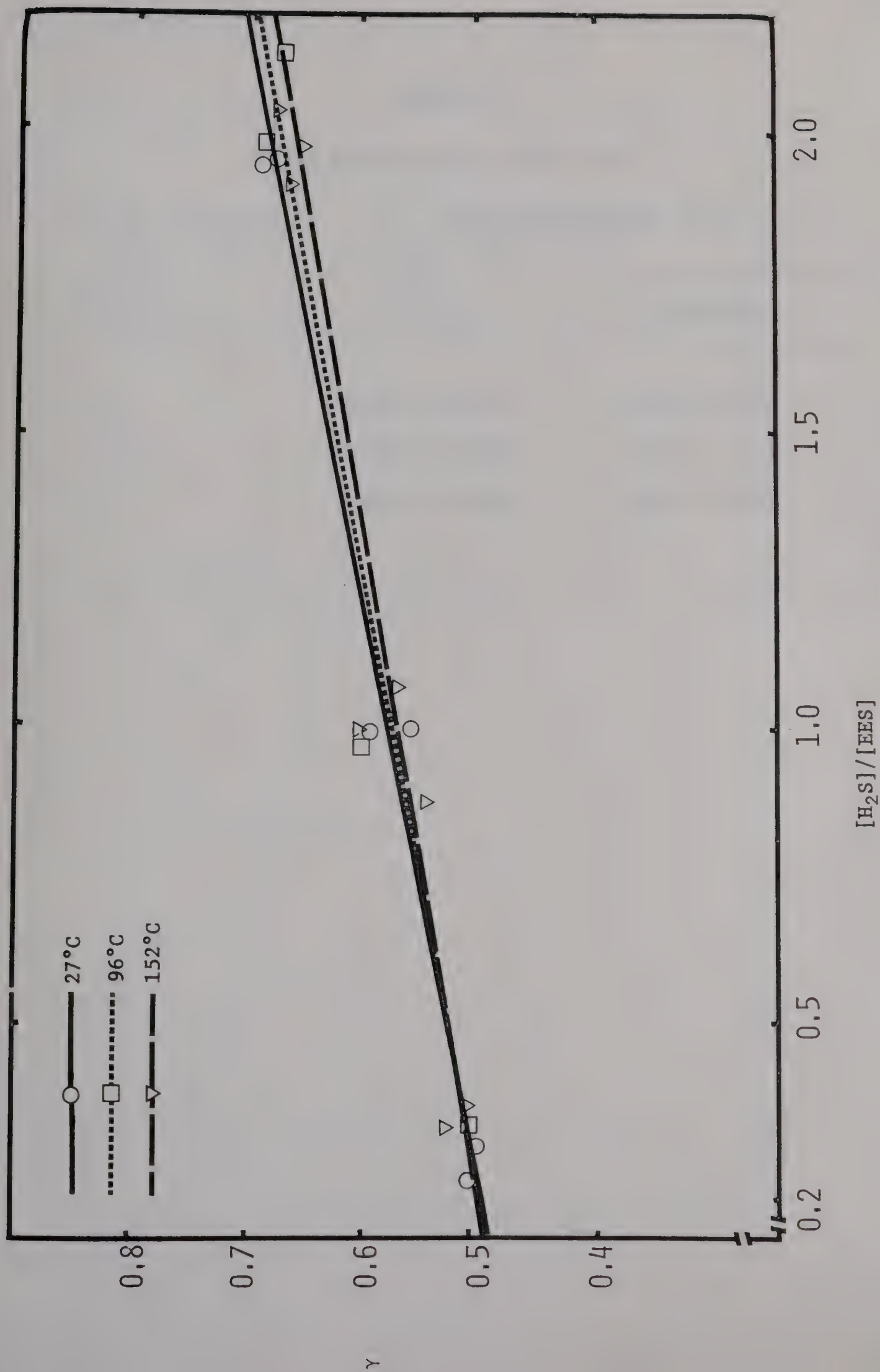


Figure 8.  $\gamma = (\phi_{C_2H_4} - k_{15a}/k_{15})^{-1}$  versus  $[H_2S]/[EES]$



TABLE XV

Slope and Intercept Values From

$$(\phi_{\text{C}_2\text{H}_4} - k_{15a}/k_{15})^{-1} = 0.5 + k_{17}[\text{H}_2\text{S}]/k_{14}[\text{EES}] \quad \text{Plots}$$

Temp., °C	$k_{17}/k_{14}$	Intercept
27	$0.101 \pm 0.006$	$0.478 \pm 0.008$
96	$0.0942 \pm 0.0082$	$0.485 \pm 0.011$
152	$0.0899 \pm 0.0051$	$0.485 \pm 0.007$



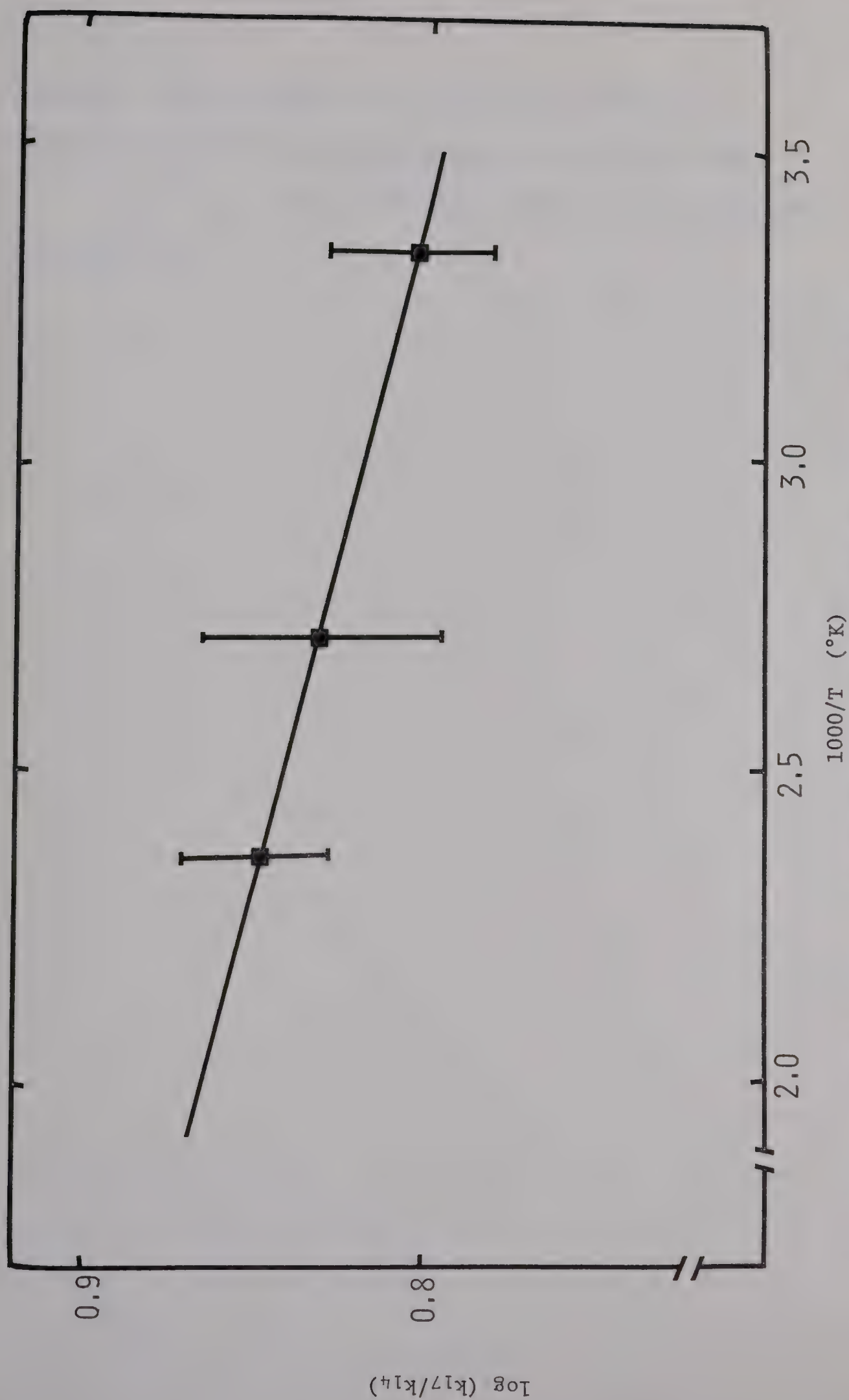


Figure 9. Arrhenius Plot for S-Abstraction from Ethylene Episulfide by H-Atoms.





Since  $E_{17} = 1709 \text{ cal mole}^{-1}$  and  $A_{17} = 12.9 \times 10^{-12} \text{ cm}^3$   
 $\text{molecule}^{-1} \text{ sec}^{-1}$  <sup>54</sup> the rate parameters for step [14] are:

$$k_{14} = (9.4 \pm 1.1) \times 10^{-11} \exp (-1944 \pm 17.5)/2.303RT \text{ cm}^3$$

$\text{molecule}^{-1} \text{ sec}^{-1}$ .



## CHAPTER IV

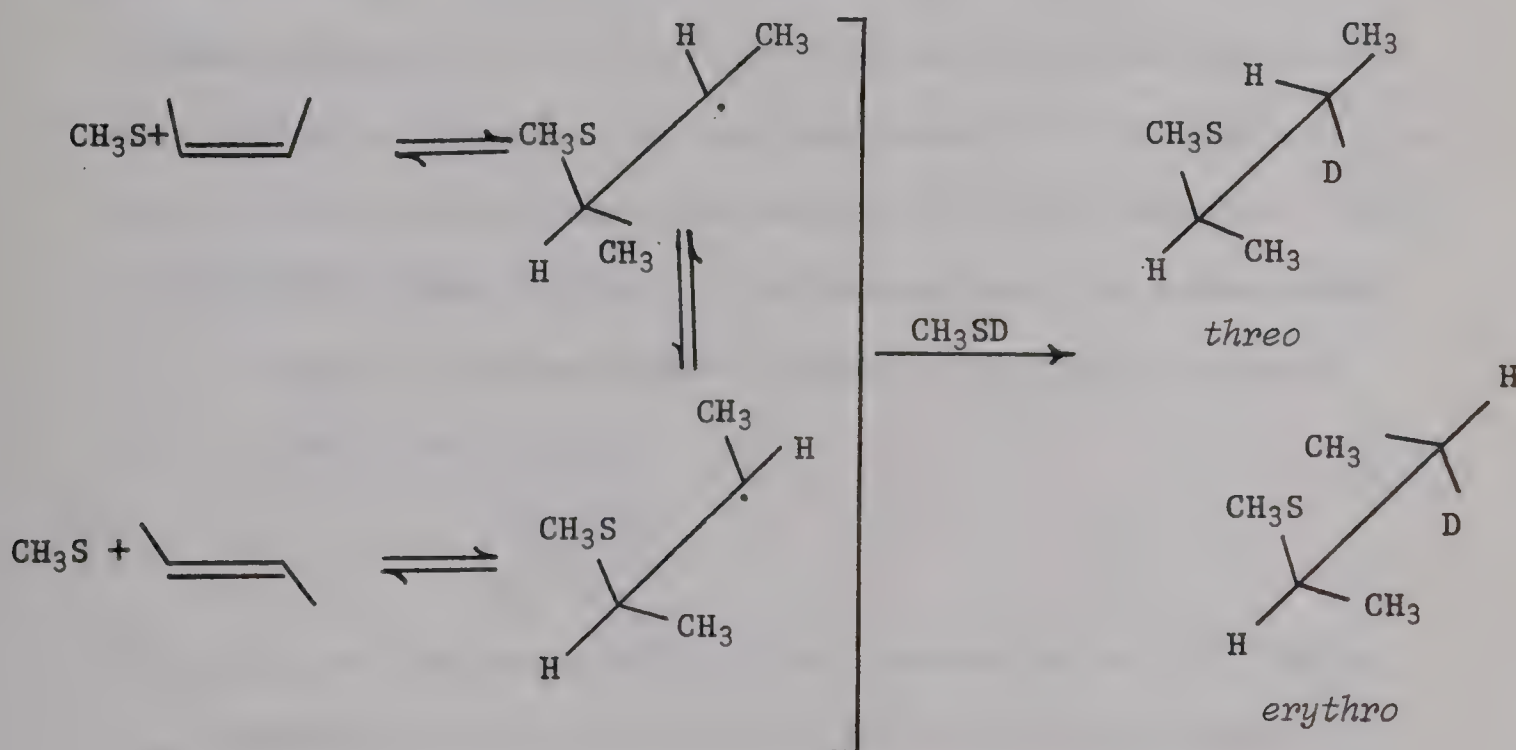
## DISCUSSION

It has been shown that methyl and methylthiyl radicals, hydrogen and sulfur atoms desulfurize episulfides very efficiently and it can be concluded that this novel reaction is of general occurrence in radical + episulfide systems. In the case of methyl radicals the simultaneous, competing, hydrogen abstraction reactions are significant because the activation energies for these processes are similar to those for sulfur abstraction. The energy barriers to desulfurization of ethylene episulfide by H or S atoms, however, are so small that this is the only observable primary process. The following kinetic and stereochemical arguments strongly point to a single step, concerted process in which the sulfur atom is transferred directly to the attacking species without the intermediacy of a thioalkyl radical.

The  $\text{CH}_3 + \text{cis-2-butene}$  episulfide system is at least 80% stereoselective and since the *cis*-2-butene product was shown to undergo rapid *cis-trans* isomerization in the presence of methyl radicals, the desulfurization reaction is probably completely stereospecific. This is in contrast to the photoinitiated addition of thiols to olefins which is a nonstereospecific process



involving the intermediacy of thioalkyl radicals<sup>59-65</sup>. The activation energies for the gas phase addition of  $\text{CH}_3\text{SH}$  to unconjugated olefins are negative and vary within the range - 5.3 to - 11.7 kcal/mole<sup>66</sup>. This, together with the observation that isomerization of the reactant olefin takes place, indicates that the initial attack of the thiyl radical on the double bond is reversible. The results of Skell and Allen<sup>63</sup> on the addition of  $\text{CH}_3\text{SD}$  to *cis*- or *trans*-2-butene are illustrative of the thiol + olefin systems:



The irradiation of  $\text{CH}_3\text{SD}$  at  $-70^\circ$  in either *cis*- or *trans*-2-butene produces a mixture of *erythro* and *threo*-3-deuterio-2-methyl-thio-butene. In the presence of  $\text{DBr}$ , however, the reaction was stereospecific with the *cis*- and *trans*-butenes yielding *threo*- and





*erythro*-3-deuterio-2-methyl-thiobutanes, respectively. In this case steric control was achieved by the rapid reaction of the thioalkyl radicals with DBr, which was faster than the radical isomerization process.

The high degree of stereoselectivity observed in the  $\text{CH}_3 + \text{cis-2-butene episulfide}$  on the other hand, militates against the intermediacy of the thioalkyl radical in this reaction. Additional arguments derived from kinetic considerations support this conclusion. The potential energy diagram for the forward and reverse processes in the  $\text{CH}_3 + \text{cis-2-butene episulfide}$  reaction is illustrated in Figure 10, and was constructed from the thermodynamic data listed in Table I and experimental activation energies. Now, if the  $\text{CH}_3\text{SCH}(\text{CH}_3)\dot{\text{C}}\text{HCH}_3$  radical is an intermediate, the unimolecular rate constant for decomposition to  $\text{CH}_3\text{S} + \text{C}_4\text{H}_8$  can be estimated from the RRK approximation,

$$k_d = A \left( \frac{E - E^*}{E} \right)^{s-1} \text{ s}^{-1}$$

where A is the pre-exponential factor, assumed to be  $10^{13}$ ,  $E^*$  is the activation energy and E is the total energy of the radical:

$$E = \Delta H_f + E_{\text{thermal}} = \Delta H_f + (s-1) RT$$

Assuming that only half the normal modes are active,

$$k_d = 10^{13} \left( \frac{29 - 15}{29} \right)^{22} = 5 \times 10^5 \text{ sec}^{-1}$$

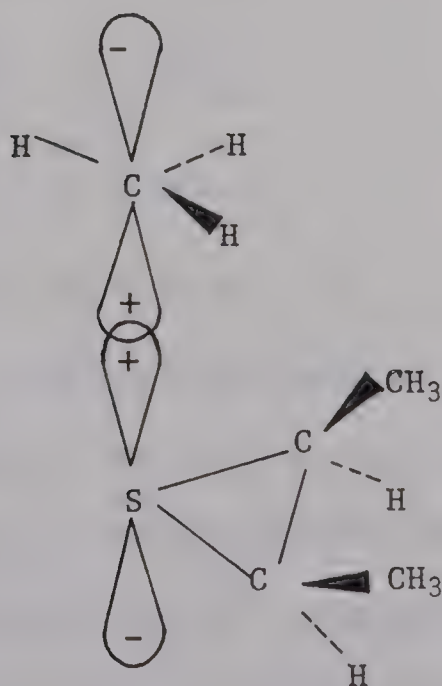






The long lifetime of the radical,  $2 \times 10^{-6}$  sec, therefore would allow ample time for *cis-trans* isomerization to take place and the butene product should be a statistical distribution of *cis* and *trans* isomers. Furthermore, collisional stabilization would be expected to compete with decomposition and the radical should undergo H-atom abstraction, either from azomethane or butene episulfide, to form a sulfide. Since neither of these processes can be inferred from the experimental results, it must be concluded that thioalkyl radicals, are not intermediates in the  $\text{CH}_3 + \text{episulfide}$  reactions.

The desulfurization of episulfides by methyl radicals must therefore follow a one-step, concerted path, the initial interaction involving the  $\pi$  orbital of the  $\text{CH}_3$  radical and the nonbonding 3p orbital of sulfur:

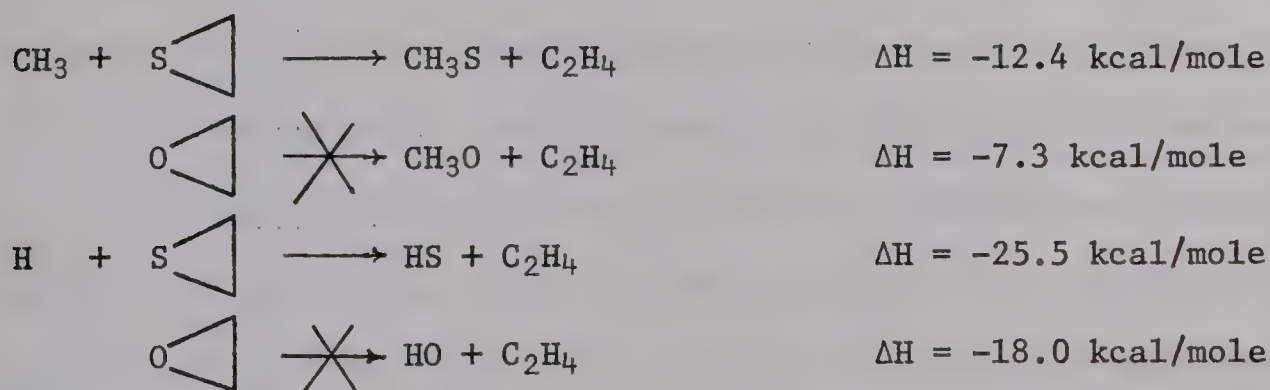






The complex may be further stabilized by back donation of charge from the carbon to sulfur d orbital. Such an intermediate is particularly significant in the context of reactivity of sulfur- and oxygen-containing molecules. Since the nonbonding 3p orbital of sulfur is more nucleophilic than the nonbonding 2p orbital of oxygen and has a higher aptitude for valence shell expansion, the  $\text{CH}_3 + \text{episulfide}$  complex should be stabilized and the activation energy consequently lowered, compared to the oxygen case. It has also been shown<sup>42</sup> that BEBO calculations predict a prohibitively high activation energy for the analogous deoxygenation reaction by methyl radicals.

The significance of d-orbital participation in desulfurization reactions is also apparent when the enthalpies of the following reactions are considered.



Obviously, the non-occurrence of deoxygenation reactions cannot be explained by enthalpy differences alone.

Semi-empirical MO calculations were carried out<sup>42</sup> on the  $\text{CH}_3 + \text{EES}$  system which should be representative of  $\text{CH}_3 + \text{episulfide}$  systems in general. Potential energies were computed by the EHMO



method<sup>67</sup> for the approach of the radical along the X, Y and Z axes using Slater-type atomic orbitals and literature values for the molecular geometries<sup>68</sup>. The calculated potential energy curve for the  $\text{CH}_3 + \text{ethylene episulfide}$  system is very complex and is illustrated in Figure 11.

The initial approach is along attractive surfaces from the Z and Y directions. The depth of the potential wells representing loose  $\text{CH}_3 \cdots \text{S} \triangleleft$  complexes is quite sizable, 7-11 kcal/mole, with the Z conformation lying lowest. As the reaction progresses the order of stability changes and in the activated complex the lowest energy barrier obtains for the Y complex with an activation energy of zero. The activation energies for the Z and X complexes are higher, having values of 3.5 and 14.5 kcal/mole, respectively. The shift in stability is probably due to the increase in steric repulsion between the methyl and ring hydrogens as the structure tightens in the activated complex. There appears to be two possible ways to reconcile the computational results with the experimental activation energy, 6.7 kcal/mole. Thus, the reaction may follow the lowest energy path and the computations systematically underestimate the heights of energy barriers or, owing to the orienting effect of the loose complex, the reaction does not follow the lowest energy path. It should be noted in this regard that the calculated enthalpy change of the reaction, -16.7 kcal/mole, compares favorably with the thermochemical value of -12.4 kcal/mole.



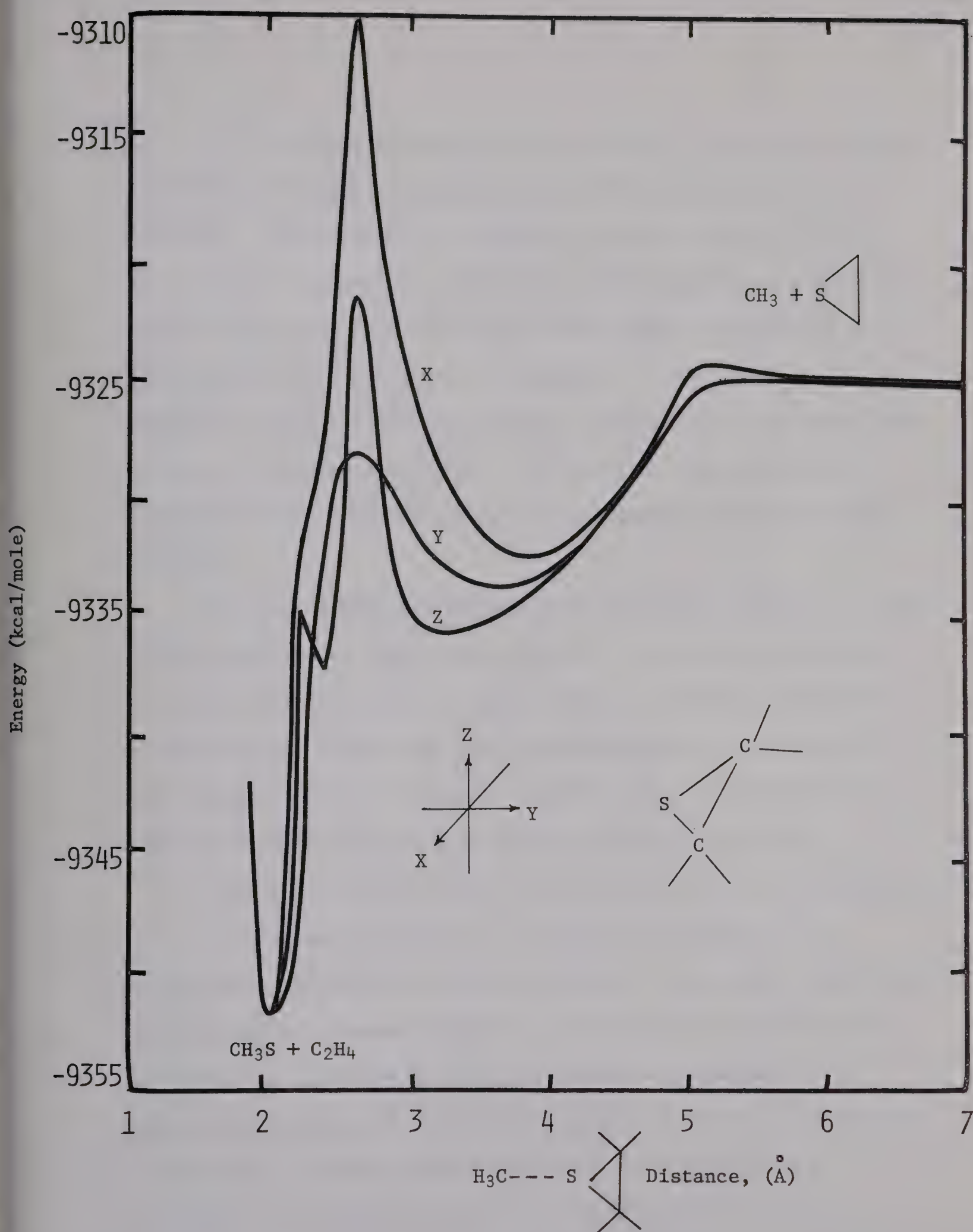


Figure 11. EHMO Potential Energy Curves for the Reaction of Methyl Radical with Ethylene Episulfide.







The Arrhenius parameters for the various S, H and CH<sub>3</sub> radical reactions with epoxides, episulfides and COS are summarized in Table XIV. For purposes of comparison, the rate data for the CH<sub>3</sub> + ethylene episulfide reaction are uncorrected for the ethylene yield arising from CH<sub>3</sub>S abstraction since similar corrections for propylene and butene could not be applied. In the ethylene episulfide case, the corrected values of log A and E<sub>a</sub> are about 10% higher and the experimental data indicate that the appropriate corrections for propylene and butene episulfide might be somewhat smaller.

For the desulfurization reaction the kinetic parameters appear to be unaffected by methyl substitution. In the butene episulfide case the reactivity may be slightly enhanced but the experimental errors here are quite large and the effect may only be illusory. The higher activation energy for the CH<sub>3</sub>S + COS  $\longrightarrow$  CH<sub>3</sub>S<sub>2</sub> + CO reaction results from the high CS bond dissociation energy:






$$D(\text{OC} = \text{S}) = 74 \text{ kcal mole}^{-1}, D(\text{C-S}) \sim 60 \text{ kcal mole}^{-1} \text{ in episulfides.}$$

The Arrhenius parameters for hydrogen abstraction from episulfides have not been determined before, nevertheless the results in Table XVI are reasonable when one considers the various factors affecting E<sub>a</sub>. Table XVII lists the Arrhenius parameters for hydrogen abstraction by methyl radicals from a variety of substrates. Intuitively, one might expect the activation energies for H-abstraction to decrease along the series EES, PES, BES line with



TABLE XVI

## Arrhenius Parameters for some Atom Transfer Reactions

	S-abstraction		H-abstraction			
	log A <sup>a</sup>	E <sub>a</sub> <sup>b</sup>	X = S		X = 0	
			log A <sup>a</sup>	E <sub>a</sub> <sup>b</sup>	log A <sup>a</sup>	E <sub>a</sub> <sup>b</sup>
CH <sub>3</sub>						
X 	11.35 ± 0.51 <sup>c</sup>	7.4 ± 0.9 <sup>c</sup>	11.34 ± 0.60 <sup>c</sup>	9.54 ± 1.00 <sup>c</sup>	-	9.6 <sup>d</sup>
X 	11.33 ± 0.92 <sup>e</sup>	7.5 ± 1.7 <sup>e</sup>	11.00 ± 0.48 <sup>e</sup>	8.26 ± 0.87 <sup>e</sup>	-	-
X 	12.31 ± 2.57 <sup>e</sup>	6.8 ± 3.9 <sup>e</sup>	11.03 ± 1.5 <sup>e</sup>	7.00 ± 2.41 <sup>e</sup>	-	-
COS	11.58 ± 0.25 <sup>c</sup>	11.4 ± 0.4 <sup>c</sup>				
H						
X 	13.75 ± <sup>e</sup>	1.9 ± 0.2 <sup>e</sup>	-	-		8.5 <sup>f</sup>
S						
X 	13.43 <sup>g</sup>	~ 0 <sup>g</sup>	-	-		
COS	13.7 <sup>h</sup>	5 <sup>h</sup>	-	-		

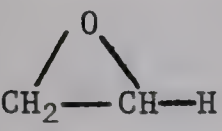
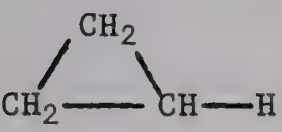
<sup>a</sup> cc mole<sup>-1</sup> sec<sup>-1</sup>; <sup>b</sup> kcal mole<sup>-1</sup>; <sup>c</sup> ref 42. Parameters for S-abstraction are not corrected for additional C<sub>2</sub>H<sub>4</sub> yields from thiyl radical abstraction. <sup>d</sup> ref. 34; <sup>e</sup> this work; <sup>f</sup> ref. 37;

<sup>g</sup> R.B. Klemm and D.D. Davis, Int. J. Chem. Kin., 5, 149(1973); <sup>h</sup> H.A.Wiebe, Ph.D. Thesis, University of Alberta, 1967.



TABLE XVII

Arrhenius Parameters for Hydrogen  
Abstraction by Methyl Radicals

Substrate	$\log A$ (cc mole <sup>-1</sup> sec <sup>-1</sup> )	$E_a$ , kcal mole <sup>-1</sup>	ref.
$\text{CH}_3(\text{C}_2\text{H}_5)\text{CH}-\text{H}$	11.87	9.5	a
$(\text{CH}_3)_3\text{C}-\text{H}$	11.38	8.03	a
	-	9.6	34
	-	13.1	b
$\text{CH}_3\text{OCH}_2-\text{H}$	11.06	9.4	c
$\text{CH}_3\text{CH}_2\text{CH}_2-\text{H}$		11.5	a

<sup>a</sup> W.M. Jackson, J.R. McNesby and B. de B. Darwent, J. Chem. Phys,

37, 1610 (1962); <sup>b</sup> J.R. McNesby & A.S. Gordon J.Amer.Chem.Soc., 79,  
825 (1957);

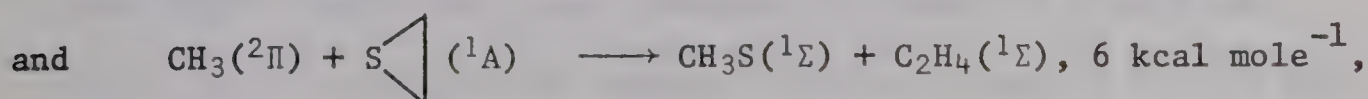
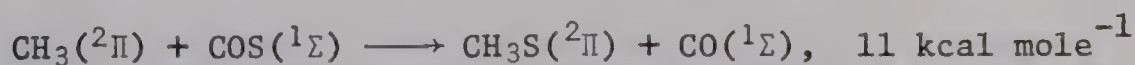
<sup>c</sup> L.F. Louks, Can. J. Chem., 45, 2775 (1967).





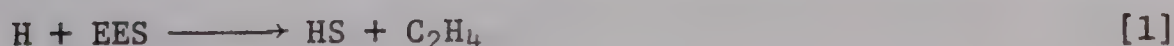
decreasing C-H bond strengths, and such a trend is actually the case. Furthermore, the molecular environment of the abstractable hydrogen atom has a great effect on its reactivity toward methyl radicals<sup>69</sup>. Adjacent oxygen atoms for example lower  $E_a$  substantially, as seen in the data for cyclopropane-ethylene oxide, and acetone-propane. Also, substitution of  $\text{CH}_3$  for H on an adjacent site lowers  $E_a$ . The present kinetic data on hydrogen abstraction from episulfides are therefore in accord with the expected trends and magnitudes.

The rate constant for sulfur abstraction from ethylene episulfide by sulfur atoms on the other hand, is close to the collision frequency and the activation energy is immeasurably small. In agreement, BEBO calculations predict a value of zero for the activation energy. The activation energies of some reactions, e.g.



however, can be reproduced with the BEBO method only if it is assumed that in order to maintain spin symmetry the S-atom transferred is in the  $^1\text{D}_2$  excited state. Owing to heavy atom perturbation some relaxation of the selection rule can occur and the experimental activation energies in fact lie between the values obtained assuming  $^3\text{P}_2$  and  $^1\text{D}_2$  atom transfer.

Hydrogen atoms also abstract sulfur from ethylene episulfide:



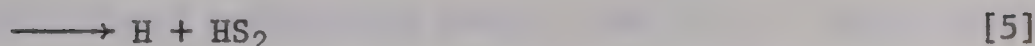


The pre-exponential factor is close to the collision frequency, as in other transfer reactions involving atoms, and the activation energy is quite small, less than 2 kcal mole<sup>-1</sup>. These values of the Arrhenius parameters appear to be consistent with those measured for the CH<sub>3</sub> + EES system, Table XVI, and the reaction



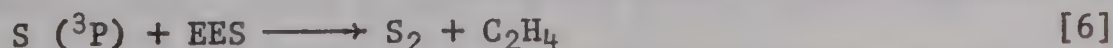
in which  $\log A = 12.95$  (cc mole<sup>-1</sup> sec<sup>-1</sup>) and  $E_a = 3.8$  kcal mole<sup>-1</sup> <sup>71</sup>.

The kinetics of the system are somewhat complicated owing to the uncertainty surrounding the fate of the sulfhydryl radical. The following reactions have been considered for the sulfhydryl radical:

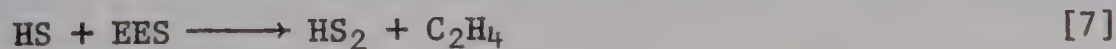


Step [5] is endothermic and consequently cannot be significant.

Since the quantum yield of hydrogen sulfide formation is 0.41 mole einstein<sup>-1</sup>, 41% of HS radicals react via step [2] leading to a quantum yield value for ethylene formation via steps [1] and [6],



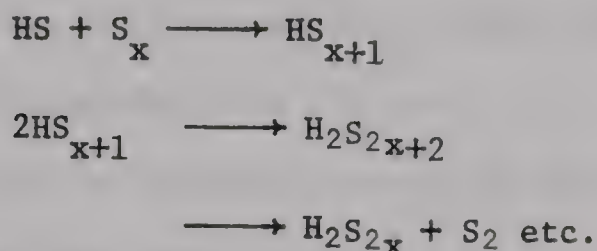
2.41. The experimental value is 2.46 and the difference, 0.05, may indicate a slow reaction between the sulfhydryl radical and episulfide,







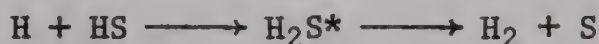
The rest of the HS radicals may disappear through steps [3] and [4], or via combination with the sulfur radicals  $S_2$ - $S_7$  present in the system:



The quantum yield of formation of  $\text{H}_2$  from the photolysis of  $\text{H}_2\text{S}$ <sup>72</sup> is 1.2 indicating that one or more  $\text{H}_2$ -forming processes take place in addition to the primary hydrogen yield from



Darwent considered reactions [2] and [3] along with



and estimated, on a qualitative basis, that 87% of the HS radicals disproportionate via step [2] and 13% via step [3]. Rommel and Schiff<sup>55</sup> also concluded, from flow experiments where the reactive intermediates were monitored by e.s.r., that step [2] is the dominant mode of decay of HS radicals, with a rate constant very close to the collision frequency. Step [3] is a four-centre reaction and therefore has a somewhat lower probability, nevertheless its occurrence has been verified by kinetic absorption spectroscopy following flash photolysis of  $\text{H}_2\text{S}$  or  $\text{H}_2\text{S}_2$ <sup>57,58</sup>. From these experiments  $k_2 + k_3$  was estimated to be ca.  $1.4 \times 10^{13} \text{ cm}^3 \text{ mole}^{-1} \text{ sec}^{-1}$ . The combination of HS radicals,

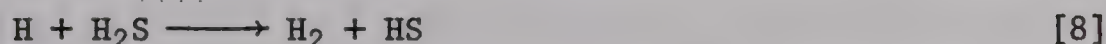






is at most, a minor process at the low pressures normally employed in flow experiments<sup>55</sup> but it could become significant at higher pressures.  $\text{H}_2\text{S}_2$  has definitely been identified in the flash photolysis of  $\text{H}_2\text{S}$ <sup>58</sup> at 30 torr.

In the determination of the Arrhenius parameters for reaction [1] using the reaction



as reference standard, the uncertainty in  $k_2/(k_2 + k_3 + Mk_4)$  will cause a slight uncertainty in the value of the Arrhenius parameters. However, since the rates of production of HS in the  $\text{H} + \text{EES}$  and  $\text{H} + \text{H}_2\text{S}$  systems are identical, the value of  $k_2/(k_2 + k_3 + Mk_4)$  should not vary noticeably with the  $\text{H}_2\text{S}$  to EES ratio and thus the kinetic relation

$$\frac{1}{\phi(\text{C}_2\text{H}_4) - k_2/(k_2 + k_3 + Mk_4)} = \frac{1}{2} + \frac{k_8}{2k_1} \cdot \frac{P[\text{H}_2\text{S}]}{P[\text{EES}]}$$

should hold reasonably well.

Finally, the entropies of activation for the metathetical reactions of  $\text{CH}_3$  radicals and H atoms with EES and  $\text{H}_2\text{S}$  were calculated from the relation

$$\Delta S^\ddagger = R \ln \left( \frac{Ah}{ekT} \right)$$

where A is the preexponential factor ( in  $1 \text{ mol}^{-1}\text{sec}^{-1}$  ),  $e = 2.718$ , h is Planck's constant and k is the Boltzmann constant. The values




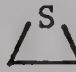
of  $\Delta S^\ddagger$  are listed in Table XVIII, where it can be seen that the entropy changes associated with methyl radicals are much greater than those effected by hydrogen atoms. This is not unexpected, owing to the large number of rocking, bending, and stretching vibrational modes in the  $\text{CH}_3$ -complex, and the A-factor is consequently lower than that for abstraction by atoms.

The overall entropy of activation consists of two contributions: an entropy decrease,  $\Delta S_1^\ddagger$ , caused by partial bond formation between the attacking species and the substrate, and an entropy increase,  $\Delta S_2^\ddagger$ , associated with structural changes and an increase in the number of normal modes in the complex. A crude estimate of the lower limit of  $\Delta S_1^\ddagger$  can be obtained from the entropy change associated with the formation of a single bond from standard entropies<sup>74</sup> using the relation  $\Delta S_c^0 = \Delta S_p^0 - R\Delta n - \Delta n R \ln RT$  where  $\Delta S_c^0$  is the entropy in molarity units,  $\Delta S_p^0$  the entropy for the standard state of one atmosphere and ideal gas, and  $\Delta n$  is the mole change of the reaction. The upper limit of  $\Delta S_2^\ddagger$  is then simply  $\Delta S^\ddagger - \Delta S_1^\ddagger$ . The various entropy changes associated with the reactions listed in Table XVIII are illustrated in Figure 12. Although the calculated values of  $\Delta S_1^\ddagger$  and  $\Delta S_2^\ddagger$  can, at best, be regarded only as rough approximations, the observed trends are probably correct. The limiting values of  $\Delta S_2^\ddagger$  correspond to the degree of alteration of the substrate in the activated complex. Accordingly, the C-S bond strengths and the frequencies of the normal modes in ethylene sulfide are drastically



TABLE XVIII

Entropies and Energies of Activation, and Preexponential Factors  
for Some Metathetical Reactions  
of Hydrogen Atoms and Methyl Radicals.

Reaction	A cc <sup>3</sup> mole <sup>-1</sup> sec <sup>-1</sup>	E <sub>a</sub> kcal mole <sup>-1</sup>	ΔS <sup>‡</sup> gibbs mole <sup>-1</sup>	Ref.
CH <sub>3</sub> +  → CH <sub>3</sub> S + C <sub>2</sub> H <sub>4</sub>	1.2 x 10 <sup>11</sup>	6.7	-23.6	42
CH <sub>3</sub> + H <sub>2</sub> S → CH <sub>4</sub> + HS	5.01 x 10 <sup>10</sup>	2.9	-25.3	73
H + H <sub>2</sub> S → HS + H <sub>2</sub>	7.8 x 10 <sup>12</sup>	1.7	-15.3	54
H +  → HS + C <sub>2</sub> H <sub>4</sub>	5.6 x 10 <sup>13</sup>	1.9	-11.4	this work





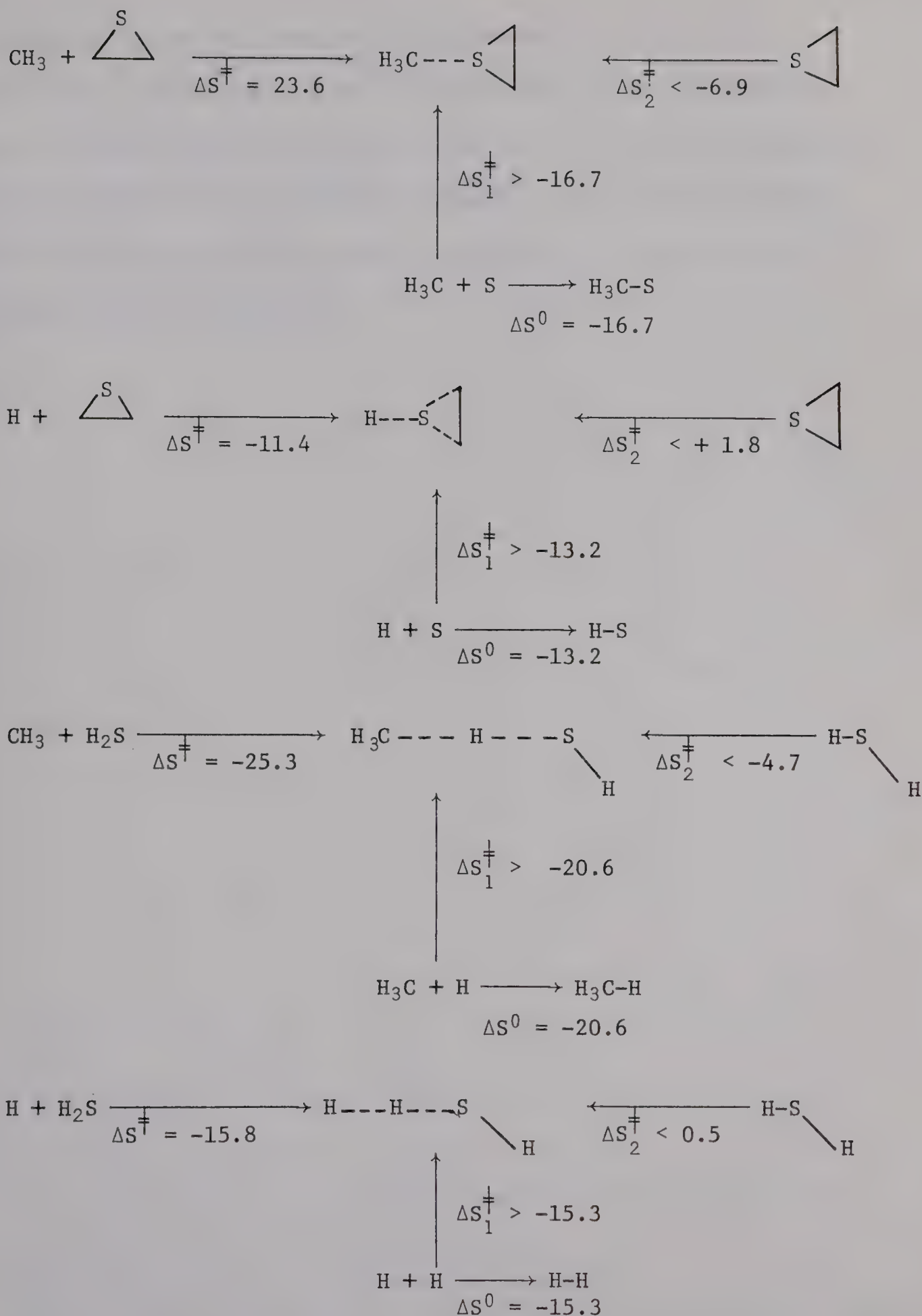


Figure 12 - Entropy changes associated with metathetical Reactions of H-Atoms and CH<sub>3</sub>-Radicals with H<sub>2</sub>S and C<sub>2</sub>H<sub>4</sub>S.



reduced in the H-atom complex, corresponding to a very loose structure. The reverse, however, takes place in the  $\text{CH}_3$  complex. The activated complexes with  $\text{H}_2\text{S}$  follow the same trend although the entropy differences are somewhat smaller. This is not surprising since ethylene episulfide would be expected to have a much more flexible structure than  $\text{H}_2\text{S}$ .



## CHAPTER V

## SUMMARY AND CONCLUSION

Methyl radicals react with episulfides via hydrogen and sulfur abstraction to yield methane and the corresponding olefin, respectively. The activation energies for desulfurization of ethylene, propylene and *cis*-2-butene episulfides are about 7 kcal mole<sup>-1</sup> and, within experimental error, do not appear to be affected by methyl substitution; the log A factors lie within the range 10.8 - 12.3 (cc mole<sup>-1</sup> sec<sup>-1</sup>). The activation energies for hydrogen abstraction decrease along the series, in line with weaker C-H bond strengths.

The reaction with *cis*-2-butene episulfide yields > 80% *cis*-2-butene and since the small yields of *trans*-2-butene were shown to arise from the methyl radical initiated *cis-trans* isomerization of the initially formed *cis* isomer, the reaction is probably stereospecific. This, together with kinetic arguments, indicates that the desulfurization reaction is a one step concerted process where the sulfur atom is transferred directly to the methyl radical without the intermediacy of thioalkyl radicals.

The analogous deoxygenation reaction with epoxides has not been observed, yet the enthalpy changes are similar to the sulfur cases. Bond energy - bond order calculations predict prohibitively





high activation energies for oxygen abstraction.

Hydrogen atoms react with ethylene episulfide exclusively via sulfur abstraction. The activation energy for this process is very small,  $1.94 \text{ kcal mole}^{-1}$ , and was determined relative to the competing hydrogen abstraction from added  $\text{H}_2\text{S}$ . In the  $\text{H} + \text{H}_2\text{S} + \text{ethylene sulfide}$  system the room temperature quantum yield of ethylene is 2.4, whereas the postulated mechanism predicts a value of 3. The discrepancy is attributed to secondary radical reactions in which HS radicals are consumed, thus preventing the disproportionation reaction,  $2\text{HS} \longrightarrow \text{H}_2\text{S} + \text{S}$  from proceeding quantitatively. Nevertheless, the form of the kinetic expression from which the Arrhenius parameters are obtained is such that the occurrence of HS consuming reactions is not expected to have a large effect on the measured values of A and  $E_a$ .



## BIBLIOGRAPHY

1. M. L. Neufeld and A.T. Blades, *Can. J. Chem.*, **41**, 3956 (1963).
2. S. W. Benson, *J. Chem. Phys.*, **40**, 105 (1964).
3. H. W. Thompson and M. Meissner, *Trans. Far. Soc.*, **32**, 1451 (1936).
4. M. C. Flowers and R. M. Parker, *J. Chem. Soc., B*, 1980 (1971)
5. E. M. Lown, H. S. Sandhu, H. E. Gunning and O. P. Strausz, *J. Am. Chem. Soc.*, **90**, 7164 (1968).
6. P. Vitins, O. P. Strausz and H. E. Gunning to be published.
7. A. Jones and F. P. Lossing, *J. Phys. Chem.*, **71**, 4111 (1967).
8. R. K. Gosavi and O. P. Strausz, to be published.
9. T.-K. Liu and A. B. F. Duncan, *J. Chem. Phys.*, **17**, 241 (1949).
10. R. Gomer and W. A. Noyes Jr., *J. Am. Chem. Soc.*, **72**, 101 (1950).
11. B. C. Roquitte, *J. Phys. Chem.*, **70**, 2699 (1966).
12. R. J. Cvetanovic, *Can. J. Chem.*, **33**, 1684 (1955).
13. R. E. Davis, *J. Org. Chem.*, **23**, 1380 (1958).
14. L. B. Clark and W. J. Simpson, *J. Chem. Phys.*, **43**, 3666 (1965).
15. D. R. Williams and L. T. Kontnik, *J. Chem. Soc., (B)*, 312 (1971).
16. A. Jackson and O. P. Strausz, to be published; K. S. Sidhu, unpublished results
17. M. J. Boskin and D. B. Denney, *Chem. Ind. (London)*, 330 (1959).
18. D. E. Bissing and A. J. Speziale, *J. Am. Chem. Soc.*, **87**, 2683 (1965).



19. A. J. Speziale and D. E. Bissing, J. Am. Chem. Soc., 85, 1888, 3878 (1963).
20. H. O. Heuse and G. Rasmusson, J. Org. Chem., 26, 4278 (1961).
21. B. Denney and M. J. Boskin, J. Am. Chem. Soc., 82, 4736 (1960).
22. R. E. Davis, J. Org. Chem., 23, 1767 (1958).
23. N. P. Neureiter and E. G. Bordwell, J. Am. Chem. Soc., 81, 578 (1958).
24. R. D. Schuetz and R. L. Jacobs, J. Org. Chem., 23, 1799 (1958).
25. F. G. Bordwell, H. M. Anderson and B. Pitt, J. Am. Chem. Soc., 76, 1082 (1954).
26. L. Paquette, Modern Heterocyclic Chemistry, W. A. Benjamin, Inc., New York 1968, p. 39.
27. S. W. Benson and W. B. de More in Ann. Revs. Phys. Chem., 16 397 (1965).
28. M. G. Evans and M. Polanyi, Trans. Faraday Soc., 32, 1933 (1936).
29. *Ibid.*, 34, 22 (1938).
30. H. S. Johnston and C. Parr, J. Am. Chem. Soc., 85, 2544 (1963).
31. H. S. Johnston, Gas Phase Reaction Rate Theory, Ronald Press, New York, 1966.
32. S. W. Mayer, J. Phys. Chem., 73, 3941 (1969).
33. S. W. Benson, "Thermochemical Kinetics", Wiley, New York, 1968, p. 97.
34. M. K. Phibbs and B. de B. Darwent, Can. J. Res., 28B, 395 (1950).
35. R. Gomer and W. A. Noyes, J. Am. Chem. Soc., 72, 101 (1950).
36. S. H. Jones and E. Whittle, Can. J. Chem., 48, 3601 (1970).





37. W. R. Trost, B. de B. Darwent and E. W. R. Steacie, *J. Chem. Phys.*, **16**, 353 (1948).
38. J. H. Plonka and P. S. Skell, *Chem. Comm.*, 1108 (1970).
39. E. Sabatino, Ph.D. Thesis, University of Connecticut, (1963).
40. K. J. Klabunde and P. S. Skell, *J. Am. Chem. Soc.*, **93**, 3807 (1971).
41. O. P. Strausz and H. E. Gunning, *Advan. Photochem.*, **4**, 143 (1966).
42. E. Jakubowski, M. G. Ahmed, E. M. Lown, H. S. Sandhu, R. K. Gosavi and O. P. Strausz, *J. Am. Chem. Soc.*, **94**, 4094 (1972).
43. R. E. Rebbert and P. Ausloos, *J. Phys. Chem.*, **67**, 1925 (1963).
44. S. Toby and J. Nimoy, *J. Phys. Chem.*, **70**, 867 (1966)
45. A. Shepp, *J. Chem. Phys.*, **24**, 939 (1956).
46. O. P. Strausz, W. B. O'Callaghan, E. M. Lown and H. E. Gunning, *J. Am. Chem. Soc.*, **93**, 559 (1971).
47. R. A. Back, *Can. J. Chem.*, **37**, 1854 (1959).
48. T. L. Pollock, Ph. D. Thesis, University of Alberta, (1971).
49. S. Searles and E. F. Lutz, *J. Am. Chem. Soc.*, **80**, 3168 (1958).
50. W. H. Carothers and F. J. Van Natta, *J. Am. Chem. Soc.*, **52**, 314 (1930).
51. P. M. Rao and A. R. Knight, *Can. J. Chem.*, **50**, 844 (1972).
52. T. Pollock, E. Jakubowski, H. E. Gunning, O. P. Strausz, *Can. J. Chem.*, **47**, 3475 (1969).
53. J. G. Calvert and J. M. Pitts Jr., *Photochemistry*, p. 74, John Wiley and Sons, New York, (1967).
54. M. J. Kurylo, N. C. Peterson and W. Braun, *J. Chem. Phys.*, **54**, 943 (1971).
55. H. Rommel and H. I. Schiff, *Int. J. Chem. Kinet.*, **4**, 547 (1972).



56. Von D. Mihelcic and R. N. Schindler, *Ber Bunsenges. Phys Chem.*, **74**, 1280 (1970).
57. P. Fowles, M. deSorgo, A. Y. Yarwood, O. P. Strausz and H. E. Gunning, *J. Am. Chem. Soc.*, **89**, 1352 (1967).
58. O. P. Strausz, R. J. Donovan and M. deSorgo, *Ber Bunsenges, Phys. Chem.*, **72**, 253 (1968).
59. F. G. Bordwell and W. A. Hewett, *J. Am. Chem. Soc.*, **79**, 3493 (1957).
60. H. L. Goering, D. I. Relyea and D. W. Larsen, *J. Am. Chem. Soc.*, **78**, 348 (1956).
61. S. J. Cristol and R. P. Arganbright, *J. Am. Chem. Soc.*, **79**, 6039 (1957).
62. C. Sivertz, *J. Phys. Chem.*, **63**, 34 (1959).
63. P. S. Skell and R. G. Allen, *J. Am. Chem. Soc.*, **82**, 1511 (1960).
64. C. Sivertz, W. Andrews, W. Elsdon and K. Graham, *J. Polym. Sci.*, **19**, 587 (1956).
65. D. M. Graham, R. L. Mieville and C. Sivertz, *Can. J. Chem.*, **42**, 2239 (1964).
66. D. M. Graham, R. L. Mieville, R. H. Pallen and C. Sivertz, *Can. J. Chem.*, **42**, 2250 (1964).
67. R. Hoffmann, *J. Chem. Phys.*, **39**, 1397 (1963).
68. Tables of Interatomic Distances and Configurations in Molecules and Ions, *Chem. Soc., Spec. Publ.*, No. 11 (1958); Suppl; No. 18 (1965).
69. P. Gray, A. A. Herod and A. Jones, *Chem. Revs.*, **71**, 247 (1971).
70. Supplementary Tables of Bimolecular Gas Reactions, E. Ratajezak and A. F. Trotman-Dickenson, Publications Department, University of Wales Institute of Science and Technology, Cardiff, Wales, 1970.
71. T. Yokota and O. P. Strausz, to be published.



72. B. de B. Darwent and R. Roberts, Proc. Roy. Soc., (London), *A216*, 344 (1953).
73. P. Gray, A. A. Herod and L. J. Leyshon, Can. J. Chem., *47*, 689 (1969).
74. S. W. Benson, Thermochemical Kinetics, Wiley, New York, 1968, pp 195-204.













**B30091**